NASA Technical Memorandum 106946

Application of the Space-Time Conservation Element and Solution Element Method to Two-Dimensional Advection-Diffusion Problems

Xiao-Yen Wang and Chuen-Yen Chow
University of Colorado
Boulder, Colorado

Sin-Chung Chang
Lewis Research Center
Cleveland, Ohio

June 1995

National Aeronautics and
Space Administration

Application of the Space-Time Conservation Element and Solution Element Method

to two-dimensional Advection-Diffusion Problems

Xiao-Yen Wang, Chuen-Yen Chow
Department of Aerospace Engineering Sciences
University of Colorado at Boulder
Boulder, Colorado 80309-0429
and
Sin-Chung Chang
National Aeronautics and Space Administration
Lewis Research Center
Cleveland, Ohio 44135

Abstract

The existing 2-D a-μ scheme and a-ϵ scheme based on the method of space-time conservation element and solution element, which were constructed for solving the linear 2-D unsteady advection-diffusion equation and unsteady advection equation, respectively, are tested here. Also, the a-ϵ scheme is modified here to become the ν-ϵ scheme for solving the nonlinear 2-D inviscid Burgers equation. Numerical solutions of six test problems are presented in comparison with their exact solutions or numerical solutions obtained by traditional finite-difference or finite-element methods. It is demonstrated that the 2-D a-μ, a-ϵ and ν-ϵ schemes can be used to obtain numerical results which are more accurate than those based on some of the traditional methods but without using any artificial tuning in the computation. Similiar to the previous 1-D test problems, the high accuracy and simplicity features of the space-time conservation element and solution element method have been revealed again in the present 2-D test results.

Introduction

The space-time conservation element and solution element (to be abbreviated as CE/SE) method is a method newly developed by Chang[1-3] for solving conservation equations describing the flow properties. The concept and methodology in this method are significantly different from those in the well-established traditional methods such as finite difference, finite volume, finite element and spectral methods. First, the flux is conserved in time and space because time and space are unified and treated equally. Second, all the dependent variables and their derivatives are considered as individual unknowns to be solved simultaneously at each grid point. And third, the concepts of conservation element (CE) and solution element (SE) are introduced to enforce both the local and global flux conservation without using any ad hoc techniques such as interpolation or extrapolation. It has been proved that this method is superior to many of the traditional methods in accuracy, simplicity and generality. Also, the stability conditions for the numerical schemes based on this method are the same as or less restrictive than those based on the traditional methods. The detailed descriptions of this method can be found in [1-3].

All of the 1-D numerical schemes constructed on the basis of CE/SE method have been tested to show that they are surperior to some traditional methods in both accuracy and stability [2,4]. Recently the two-dimensional versions of the a-μ scheme, a-ϵ scheme and Euler solver have also been constructed by Chang [3] based on the same set of design principles.

In this work, the aforementioned 2-D schemes and an extended scheme are tested using several model problems. The 2-D unsteady advection-diffusion equation is solved by use of the a-μ scheme. The influence of diffusivity on the accuracy of the numerical solution is investigated by comparing with the exact solution. The 2-D pure advection equation is solved using the a-ϵ scheme with varying ϵ to study its effect on numerical diffusion. Then the 2-D pure diffusion equation is solved using the μ scheme, which is a special form of the a-μ scheme by letting $a_x = a_y = 0$. The numerical results are compared with those obtained by Crank-Nicolson implicit finite-difference and finite-element methods. Furthermore, the a-ϵ scheme is modified to become the ν-ϵ scheme for inviscid Burgers equation. Two test problems are used to demonstrate that the ν-ϵ scheme is still more effective than several traditional finite-difference methods in solving nonlinear problems in a much simpler manner.

Numerical Schemes

1. The a-μ Scheme for Advection-Diffusion Equation

The basic a-μ scheme is first reviewed, which is constructed for solving the linear advection-diffusion equation

$$\frac{\partial u}{\partial t} + a_x \frac{\partial u}{\partial x} + a_y \frac{\partial u}{\partial y} = \mu(\frac{\partial^2 u}{\partial x^2} + \frac{\partial^2 u}{\partial y^2}) \tag{1.1}$$

where a_x and a_y are the constant advection speeds and μ is the viscosity coefficient. In the space-time Euclidean space E_3, the integral form of (1.1) is

$$\int\int_V (\nabla \cdot \vec{h}) dV = 0 \tag{1.2}$$

where $\vec{h} = (a_x u - \mu \partial u/\partial x, a_y u - \mu \partial u/\partial y, u)$ and V is an arbitrary space-time region in E_3. By use of Gauss' divergence theorem, Eq. (1.2) becomes

$$\oint_{S(V)} \vec{h} \cdot d\vec{s} = 0 \tag{1.3}$$

where $S(V)$ is the boundary of region V and $d\vec{s} = d\sigma \vec{n}$ with $d\sigma$ and $\vec{n}$, respectively, being the area and the outward unit normal of a surface element on $S(V)$.

The conservation element (CE) and solution element (SE) are the two basic elements used in the construction of numerical schemes. Some representative CE(j,n) and SE(j,n) are depicted in Fig. 1. There are two sets of mesh points (j,k,n) where j and k are spatial mesh indices and n is the time mesh index(see Fig. 1(a)). One of which, denoted as Ω_1, is the set of solid circles with $j,k = 0, \pm 1, \pm 2, \cdots$ and $n = \pm 1/2, \pm 3/2, \pm 5/2, \cdots$. The other denoted as Ω_2, is the set of harrow circles with $j,k = 1/3, 1/3 \pm 1, 1/3 \pm 2, \cdots$ and $n = 0, \pm 1, \pm 2, \cdots$. Each mesh point (j,k,n) in Ω_1 or Ω_2 is associated with three CEs, which are quadrilateral cylinders in space-time, one SE, which is the union of three vertical planes, a horizontal plane, and their immediate neighborhood. The CEs and SEs in Ω_1, denoted as $\text{CE}_l^{(1)}(j,k,n+1/2), l = 1,2,3$ and $\text{SE}^{(1)}(j,k,n+1/2)$(see Fig. 1(b)(c)), are different from those in Ω_2, denoted as $\text{CE}_l^{(1)}(j,k,n+1), l = 1,2,3$ and $\text{SE}^{(2)}(j,k,n+1)$(see Fig. 1(d)(e)). The geometry of the hexagon $ABCDEF$, which appears in the CEs(SEs) at the mesh points $(j,k,n) \in$ both Ω_1 and Ω_2 , is determined by three positive parameters w, b and h(see Fig. 1(f)).

For any $(j,k,n) \in \Omega$, let

$$SE(j,k,n) = \begin{cases} SE^{(1)}(j,k,n), & \text{if} \quad (j,k,n) \in \Omega_1 \\ SE^{(2)}(j,k,n), & \text{if} \quad (j,k,n) \in \Omega_2 \end{cases} \tag{1.4}$$

For any $(x,y,t) \in \mathrm{SE}(j,k,n)$, $u(x,y,t)$ and $\vec{h}(x,y,t)$ are approximated by

$$u^*(x,y,t;j,k,n) = u^n_{j,k} + (u_x)^n_{j,k}(x - x_{j,k}) + (u_y)^n_{j,k}(y - y_{j,k}) + (u_t)^n_{j,k}(t - t^n) \tag{1.5}$$

and

$$\vec{h}^*(x,y,t;j,k,n) = [\, a_x u^*(x,y,t;j,k,n) - \mu \partial u^*(x,y,t;j,k,n)/\partial x,$$
$$a_y u^*(x,y,t;j,k,n) - \mu \partial u^*(x,y,t;j,k,n)/\partial y,\ u^*(x,y,t;j,k,n)\,] \tag{1.6}$$

where $u^n_{j,k}, (u_x)^n_{j,k}, (u_y)^n_{j,k}$ and $(u_t)^n_{j,k}$ are constant within $\mathrm{SE}(j,k,n)$. The assumption that $u = u^*(x,y,t;j,k,n)$ satisfies (1.1) implies

$$(u_t)^n_{j,k} = -\left[a_x (u_x)^n_{j,k} + a_y (u_y)^n_{j,k}\right] \tag{1.7}$$

Substituting (1.7) into (1.5), one has

$$u^*(x,y,t;j,k,n) = u^n_{j,k} + (u_x)^n_{j,k}[(x - x_{j,k}) - a_x(t - t^n)] + (u_y)^n_{j,k}[(y - y_{j,k}) - a_y(t - t^n)] \tag{1.8}$$

Thus there are three independent marching variables, i.e., $u^n_{j,k}, (u_x)^n_{j,k}, (u_y)^n_{j,k}$ associated with a mesh point $(j,k,n) \in \Omega$.

Considering (1.3) in any arbitrary $\mathrm{CE}^{(1)}_l(j,k,n+1/2) \in \Omega_1$, the approximation is

$$\oint_{S(CE^{(1)}_l(j,k,n+1/2))} \vec{h}^* \cdot d\vec{s} = 0, \quad l = 1,2,3 \tag{1.9}$$

Similarly, in any arbitrary $\mathrm{CE}^{(2)}_l(j,k,n+1) \in \Omega_2$, the approximation is

$$\oint_{S(CE^{(2)}_l(j,k,n+1))} \vec{h}^* \cdot d\vec{s} = 0, \quad l = 1,2,3 \tag{1.10}$$

As a preliminary for the evaluation of the integrals (1.9) and (1.10), a new coordinate system (ζ,η) shown in Fig. 1(f) is introduced. Some transformed coefficients in the (ζ,η) coordinate which will be used in the following computations are described briefly as following:

$$\begin{pmatrix} x \\ y \end{pmatrix} = T \begin{pmatrix} \zeta \\ \eta \end{pmatrix}, \quad \begin{pmatrix} a_\zeta \\ a_\eta \end{pmatrix} = T^{-1} \begin{pmatrix} a_x \\ a_y \end{pmatrix}, \quad \begin{pmatrix} u_\zeta \\ u_\eta \end{pmatrix} = T^t \begin{pmatrix} u_x \\ u_y \end{pmatrix} \tag{1.11}$$

where

$$T = \begin{pmatrix} \dfrac{w-b}{\Delta\zeta} & \dfrac{w+b}{\Delta\eta} \\ -\dfrac{h}{\Delta\zeta} & \dfrac{h}{\Delta\eta} \end{pmatrix} \quad T^{-1} = \begin{pmatrix} \dfrac{\Delta\zeta}{2w} & -\dfrac{(w+b)\Delta\zeta}{2wh} \\ \dfrac{\Delta\eta}{2w} & \dfrac{(w-b)\Delta\eta}{2wh} \end{pmatrix} \tag{1.12}$$

with

$$\Delta\zeta = \sqrt{(w-b)^2+h^2}, \quad \Delta\eta = \sqrt{(w+b)^2+h^2} \tag{1.13}$$

and T^t is the transpose of T. Let

$$u_\zeta^+ = \frac{\Delta\zeta}{6}u_\zeta, \quad u_\eta^+ = \frac{\Delta\eta}{6}u_\eta \tag{1.14}$$

$$\nu_\zeta = \frac{3}{2}\frac{\Delta t}{\Delta\zeta}a_\zeta, \quad \nu_\eta = \frac{3}{2}\frac{\Delta t}{\Delta\eta}a_\eta \tag{1.15}$$

and

$$\xi_\zeta = \frac{9\mu\Delta t}{8w^2h^2}(\Delta\zeta)^2, \quad \xi_\eta = \frac{9\mu\Delta t}{8w^2h^2}(\Delta\eta)^2, \quad \xi_\tau = \frac{9\mu\Delta t}{8w^2h^2}(\Delta\tau)^2 \tag{1.16}$$

where $\Delta\tau = 2\sqrt{b^2+h^2}$. Furthermore, let $\sigma_{11}^{(1)+}, \sigma_{11}^{(1)-}, \cdots$ be defined by

$$\begin{aligned}
\sigma_{11}^{(1)\pm} &= 1-\nu_\zeta-\nu_\eta && (1.17)\\
\sigma_{12}^{(1)\pm} &= \pm(1-\nu_\zeta-\nu_\eta)(1+\nu_\zeta)+\xi_\eta+\xi_\tau-\xi_\zeta && (1.18)\\
\sigma_{13}^{(1)\pm} &= \pm(1-\nu_\zeta-\nu_\eta)(1+\nu_\eta)+\xi_\zeta+\xi_\tau-\xi_\eta && (1.19)\\
\sigma_{21}^{(1)\pm} &= 1+\nu_\zeta && (1.20)\\
\sigma_{22}^{(1)\pm} &= \mp(1+\nu_\zeta)(2-\nu_\zeta)-2\xi_\eta && (1.21)\\
\sigma_{23}^{(1)\pm} &= \pm(1+\nu_\zeta)(1+\nu_\eta)+\xi_\zeta-\xi_\tau+\xi_\eta && (1.22)\\
\sigma_{31}^{(1)\pm} &= 1+\nu_\eta && (1.23)\\
\sigma_{32}^{(1)\pm} &= \pm(1+\nu_\eta)(1+\nu_\zeta)+\xi_\zeta-\xi_\tau+\xi_\eta && (1.24)\\
\sigma_{33}^{(1)\pm} &= \mp(1+\nu_\eta)(2-\nu_\eta)-2\xi_\zeta && (1.25)\\
\sigma_{11}^{(2)\pm} &= 1+\nu_\zeta+\nu_\eta && (1.26)\\
\sigma_{12}^{(2)\pm} &= \mp(1+\nu_\zeta+\nu_\eta)(1-\nu_\zeta)-\xi_\eta-\xi_\tau+\xi_\zeta && (1.27)\\
\sigma_{13}^{(2)\pm} &= \mp(1+\nu_\zeta+\nu_\eta)(1-\nu_\eta)-\xi_\zeta-\xi_\tau+\xi_\eta && (1.28)\\
\sigma_{21}^{(2)\pm} &= 1-\nu_\zeta && (1.29)\\
\sigma_{22}^{(2)\pm} &= \pm(1-\nu_\zeta)(2+\nu_\zeta)+2\xi_\eta && (1.30)\\
\sigma_{23}^{(2)\pm} &= \mp(1-\nu_\zeta)(1-\nu_\eta)-\xi_\zeta+\xi_\tau-\xi_\eta && (1.31)\\
\sigma_{31}^{(2)\pm} &= 1-\nu_\eta && (1.32)\\
\sigma_{32}^{(2)\pm} &= \mp(1-\nu_\eta)(1-\nu_\zeta)-\xi_\zeta+\xi_\tau-\xi_\eta && (1.33)\\
\sigma_{33}^{(2)\pm} &= \pm(1-\nu_\eta)(2+\nu_\eta)+2\xi_\zeta && (1.34)
\end{aligned}$$

With the above definitions, the final results of (1.9) and (1.10) are:

$$\left[\sigma_{11}^{(1)+}u+\sigma_{12}^{(1)+}u_\zeta^+ +\sigma_{13}^{(1)+}u_\eta^+\right]_{j,k}^{n+1/2} = \left[\sigma_{11}^{(1)-}u+\sigma_{12}^{(1)-}u_\zeta^+ +\sigma_{13}^{(1)-}u_\eta^+\right]_{j+1/3,k+1/3}^{n} \tag{1.35}$$

$$\left[\sigma_{21}^{(1)+}u+\sigma_{22}^{(1)+}u_\zeta^+ +\sigma_{23}^{(1)+}u_\eta^+\right]_{j,k}^{n+1/2} = \left[\sigma_{21}^{(1)-}u+\sigma_{22}^{(1)-}u_\zeta^+ +\sigma_{23}^{(1)-}u_\eta^+\right]_{j-2/3,k+1/3}^{n} \tag{1.36}$$

$$\left[\sigma_{31}^{(1)+}u+\sigma_{32}^{(1)+}u_\zeta^+ +\sigma_{33}^{(1)+}u_\eta^+\right]_{j,k}^{n+1/2} = \left[\sigma_{31}^{(1)-}u+\sigma_{32}^{(1)-}u_\zeta^+ +\sigma_{33}^{(1)-}u_\eta^+\right]_{j+1/3,k-2/3}^{n} \tag{1.37}$$

$$\left[\sigma_{11}^{(2)+}u+\sigma_{12}^{(2)+}u_\zeta^+ +\sigma_{13}^{(2)+}u_\eta^+\right]_{j,k}^{n+1} = \left[\sigma_{11}^{(2)-}u+\sigma_{12}^{(2)-}u_\zeta^+ +\sigma_{13}^{(2)-}u_\eta^+\right]_{j-1/3,k-1/3}^{n+1/2} \tag{1.38}$$

$$\left[\sigma_{21}^{(2)+}u+\sigma_{22}^{(2)+}u_\zeta^+ +\sigma_{23}^{(2)+}u_\eta^+\right]_{j,k}^{n+1} = \left[\sigma_{21}^{(2)-}u+\sigma_{22}^{(2)-}u_\zeta^+ +\sigma_{23}^{(2)-}u_\eta^+\right]_{j+2/3,k-1/3}^{n+1/2} \tag{1.39}$$

$$\left[\sigma_{31}^{(2)+}u+\sigma_{32}^{(2)+}u_\zeta^+ +\sigma_{33}^{(2)+}u_\eta^+\right]_{j,k}^{n+1} = \left[\sigma_{31}^{(2)-}u+\sigma_{32}^{(2)-}u_\zeta^+ +\sigma_{33}^{(2)-}u_\eta^+\right]_{j-1/3,k+2/3}^{n+1/2} \tag{1.40}$$

Let $s_1^{(1)}, s_2^{(1)}, s_3^{(1)}, s_1^{(2)}, s_2^{(2)}$, and $s_3^{(2)}$ denote the expressions on the right sides of (1.35)-(1.40), respectively, and

$$\begin{aligned}
\rho_{21}^{(1)} &= [3(1+\nu_\zeta)(1+\nu_\eta)+(3+2\nu_\zeta+\nu_\eta)\xi_\zeta+(1+\nu_\eta)(\xi_\eta-\xi_\tau)]/\Delta^{(1)} && (1.41)\\
\rho_{22}^{(1)} &= [-3(1+\nu_\eta)(1-\nu_\zeta-\nu_\eta)-(3-2\nu_\zeta-\nu_\eta)\xi_\zeta+(1+\nu_\eta)(\xi_\eta-\xi_\tau)]/\Delta^{(1)} && (1.42)\\
\rho_{23}^{(1)} &= [(2\nu_\zeta+\nu_\eta)\xi_\zeta+(2-\nu_\eta)(\xi_\tau-\xi_\eta)]/\Delta^{(1)} && (1.43)\\
\rho_{31}^{(1)} &= [3(1+\nu_\zeta)(1+\nu_\eta)+(3+\nu_\zeta+2\nu_\eta)\xi_\eta+(1+\nu_\zeta)(\xi_\zeta-\xi_\tau)]/\Delta^{(1)} && (1.44)\\
\rho_{32}^{(1)} &= [(\nu_\zeta+2\nu_\eta)\xi_\eta+(2-\nu_\zeta)(\xi_\tau-\xi_\zeta)]/\Delta^{(1)} && (1.45)\\
\rho_{33}^{(1)} &= [-3(1+\nu_\zeta)(1-\nu_\zeta-\nu_\eta)-(3-\nu_\zeta-2\nu_\eta)\xi_\eta+(1+\nu_\zeta)(\xi_\zeta-\xi_\tau)]/\Delta^{(1)} && (1.46)\\
\rho_{21}^{(2)} &= [-3(1-\nu_\zeta)(1-\nu_\eta)-(3-2\nu_\zeta-\nu_\eta)\xi_\zeta+(1-\nu_\eta)(\xi_\tau-\xi_\eta)]/\Delta^{(2)} && (1.47)\\
\rho_{22}^{(2)} &= [3(1-\nu_\eta)(1+\nu_\zeta+\nu_\eta)+(3+2\nu_\zeta+\nu_\eta)\xi_\zeta+(1-\nu_\eta)(\xi_\tau-\xi_\eta)]/\Delta^{(2)} && (1.48)\\
\rho_{23}^{(2)} &= [(2\nu_\zeta+\nu_\eta)\xi_\zeta+(2+\nu_\eta)(-\xi_\tau+\xi_\eta)]/\Delta^{(2)} && (1.49)\\
\rho_{31}^{(2)} &= [-3(1-\nu_\zeta)(1-\nu_\eta)-(3-\nu_\zeta-2\nu_\eta)\xi_\eta+(1-\nu_\zeta)(-\xi_\zeta+\xi_\tau)]/\Delta^{(2)} && (1.50)\\
\rho_{32}^{(2)} &= [(\nu_\zeta+2\nu_\eta)\xi_\eta+(2+\nu_\zeta)(-\xi_\tau+\xi_\zeta)]/\Delta^{(2)} && (1.51)\\
\rho_{33}^{(2)} &= [3(1-\nu_\zeta)(1+\nu_\zeta+\nu_\eta)+(3+\nu_\zeta+2\nu_\eta)\xi_\eta+(1-\nu_\zeta)(\xi_\tau-\xi_\zeta)]/\Delta^{(2)} && (1.52)
\end{aligned}$$

where

$$\begin{aligned}
\Delta^{(1)} &= 3\,[3(1+\nu_\zeta)(1+\nu_\eta)(1-\nu_\zeta-\nu_\eta)+2(1+\nu_\zeta)(1-\nu_\zeta-\nu_\eta)\xi_\zeta\\
&\quad +2(1+\nu_\eta)(1-\nu_\zeta-\nu_\eta)\xi_\eta+2(1+\nu_\zeta)(1+\nu_\eta)\xi_\tau+\left(\frac{9\mu\Delta t}{2wh}\right)^2\Big] && (1.53)
\end{aligned}$$

$$\Delta^{(2)} = 3\left[3(1-\nu_\zeta)(1-\nu_\eta)(1+\nu_\zeta+\nu_\eta)+2(1-\nu_\zeta)(1+\nu_\zeta+\nu_\eta)\xi_\zeta \right. \\ \left. +2(1-\nu_\eta)(1+\nu_\zeta+\nu_\eta)\xi_\eta+2(1-\nu_\zeta)(1-\nu_\eta)\xi_\tau+\left(\frac{9\mu\Delta t}{2wh}\right)^2\right] \quad (1.54)$$

With the assumption of $\Delta^{(1)} \neq 0$ and $\Delta^{(2)} \neq 0$, the final form of the a-μ scheme are

$$u_{j,k}^{n+1/2} = \left[s_1^{(1)} + s_2^{(1)} + s_3^{(1)}\right]/3 \quad (1.55)$$

$$(u_\zeta^+)_{j,k}^{n+1/2} = \rho_{21}^{(1)} s_1^{(1)} + \rho_{22}^{(1)} s_2^{(1)} + \rho_{23}^{(1)} s_3^{(1)} \quad (1.56)$$

$$(u_\eta^+)_{j,k}^{n+1/2} = \rho_{31}^{(1)} s_1^{(1)} + \rho_{32}^{(1)} s_2^{(1)} + \rho_{33}^{(1)} s_3^{(1)} \quad (1.57)$$

where $(j,k,n+1/2) \in \Omega_1$, and

$$u_{j,k}^{n+1} = \left[s_1^{(2)} + s_2^{(2)} + s_3^{(2)}\right]/3 \quad (1.58)$$

$$(u_\zeta^+)_{j,k}^{n+1} = \rho_{21}^{(2)} s_1^{(2)} + \rho_{22}^{(2)} s_2^{(2)} + \rho_{23}^{(2)} s_3^{(2)} \quad (1.59)$$

$$(u_\eta^+)_{j,k}^{n+1} = \rho_{31}^{(2)} s_1^{(2)} + \rho_{32}^{(2)} s_2^{(2)} + \rho_{33}^{(2)} s_3^{(2)} \quad (1.60)$$

where $(j,k,n+1) \in \Omega_2$.

The a-μ scheme is second-order accurate in space and time. Detailed derivations and discussions of the stability condition for the a-μ scheme are referred to [3].

2. The a-ϵ Scheme for Unsteady Advection Equation

Equation (1.1) becomes the pure advection equation

$$\frac{\partial u}{\partial t} + a_x \frac{\partial u}{\partial x} + a_y \frac{\partial u}{\partial y} = 0 \quad (2.1)$$

when $\mu = 0$. It is expected that the a-μ scheme may become unstable as $\mu \to 0$ for the nonlinear problems. Some modifications are thus needed for its improvement. The CEs in the a-μ scheme are replaced by

$$CE^{(1)}(j,k,n+1/2) \\ = \left[CE_1^{(1)}(j,k,n+1/2)\right] \cup \left[CE_2^{(1)}(j,k,n+1/2)\right] \cup \left[CE_3^{(1)}(j,k,n+1/2)\right] \quad (2.2)$$

where $(j,k,n+1/2) \in \Omega_1$, and

$$CE^{(2)}(j,k,n+1) \\ = \left[CE_1^{(2)}(j,k,n+1)\right] \cup \left[CE_2^{(2)}(j,k,n+1)\right] \cup \left[CE_3^{(2)}(j,k,n+1)\right] \quad (2.3)$$

where $(j,k,n+1) \in \Omega_2$. The total flux leaving the boundary of any new CE is assumed to be zero, i.e.,

$$\oint_{S(CE^{(1)}(j,k,n+1/2))} \vec{h}^* \cdot d\vec{s} = 0 \tag{2.4}$$

and

$$\oint_{S(CE^{(2)}(j,k,n+1))} \vec{h}^* \cdot d\vec{s} = 0 \tag{2.5}$$

Substituting (1.17)–(1.34) into (1.35)–(1.40) with $\xi_\zeta = \xi_\eta = \xi_\tau = 0$, one obtains

$$\left[u + (1+\nu_\zeta)u_\zeta^+ + (1+\nu_\eta)u_\eta^+\right]_{j,k}^{n+1/2} = \left[u - (1+\nu_\zeta)u_\zeta^+ - (1+\nu_\eta)u_\eta^+\right]_{j+1/3,k+1/3}^{n} \tag{2.6}$$

$$\left[u - (2-\nu_\zeta)u_\zeta^+ + (1+\nu_\eta)u_\eta^+\right]_{j,k}^{n+1/2} = \left[u + (2-\nu_\zeta)u_\zeta^+ - (1+\nu_\eta)u_\eta^+\right]_{j-2/3,k+1/3}^{n} \tag{2.7}$$

$$\left[u + (1+\nu_\zeta)u_\zeta^+ - (2-\nu_\eta)u_\eta^+\right]_{j,k}^{n+1/2} = \left[u - (1+\nu_\zeta)u_\zeta^+ + (2-\nu_\eta)u_\eta^+\right]_{j+1/3,k-2/3}^{n} \tag{2.8}$$

$$\left[u - (1-\nu_\zeta)u_\zeta^+ - (1-\nu_\eta)u_\eta^+\right]_{j,k}^{n+1} = \left[u + (1-\nu_\zeta)u_\zeta^+ + (1-\nu_\eta)u_\eta^+\right]_{j-1/3,k-1/3}^{n+1/2} \tag{2.9}$$

$$\left[u + (2+\nu_\zeta)u_\zeta^+ - (1-\nu_\eta)u_\eta^+\right]_{j,k}^{n+1} = \left[u - (2+\nu_\zeta)u_\zeta^+ + (1-\nu_\eta)u_\eta^+\right]_{j+2/3,k-1/3}^{n+1/2} \tag{2.10}$$

$$\left[u - (1-\nu_\zeta)u_\zeta^+ + (2+\nu_\eta)u_\eta^+\right]_{j,k}^{n+1} = \left[u + (1-\nu_\zeta)u_\zeta^+ - (2+\nu_\eta)u_\eta^+\right]_{j-1/3,k+2/3}^{n+1/2} \tag{2.11}$$

when $|\nu_\zeta| \neq 1, |\nu_\eta| \neq 1$ and $|\nu_\zeta + \nu_\eta| \neq 1$. Let $\acute{s}_1^{(1)}, \acute{s}_2^{(1)}, \acute{s}_3^{(1)}, \acute{s}_1^{(2)}, \acute{s}_2^{(2)}$, and $\acute{s}_3^{(2)}$ denote the expressions on the right sides of (2.6)–(2.11), respectively. From (2.6)–(2.8) and (2.9)–(2.11), respectively, one obtains

$$u_{j,k}^{n+1/2} = \frac{1}{3}\left[(1-\nu_\zeta-u_\eta)\acute{s}_1^{(1)} + (1+\nu_\zeta)\acute{s}_2^{(1)} + (1+\nu_\eta)\acute{s}_3^{(1)}\right] \tag{2.12}$$

$$(u_\zeta^{\circ+})_{j,k}^{n+1/2} = \frac{1}{3}\left[\acute{s}_1^{(1)} - \acute{s}_2^{(1)}\right] \tag{2.13}$$

$$(u_\eta^{\circ+})_{j,k}^{n+1/2} = \frac{1}{3}\left[\acute{s}_1^{(1)} - \acute{s}_3^{(1)}\right] \tag{2.14}$$

where $(j,k,n+1/2) \in \Omega_1$, and

$$u_{j,k}^{n+1} = \frac{1}{3}\left[(1+\nu_\zeta+u_\eta)\acute{s}_1^{(2)} + (1-\nu_\zeta)\acute{s}_2^{(2)} + (1-\nu_\eta)\acute{s}_3^{(2)}\right] \tag{2.15}$$

$$(u_\zeta^{\circ+})_{j,k}^{n+1} = \frac{1}{3}\left[\acute{s}_2^{(2)} - \acute{s}_1^{(2)}\right] \tag{2.16}$$

$$(u_\eta^{\circ+})_{j,k}^{n+1} = \frac{1}{3}\left[\acute{s}_3^{(2)} - \acute{s}_1^{(2)}\right] \tag{2.17}$$

where $(j,k,n+1) \in \Omega_2$.

For any $(j,k,n+1/2)\in\Omega_1$, the numerical analogues of $(u_\zeta^+)_{j,k}^{n+1/2}$ and $(u_\eta^+)_{j,k}^{n+1/2}$ using the central-difference approximation are defined as

$$(u_\zeta'^+)_{j,k}^{n+1/2}=(u'^{n+1/2}_{j+1/3,k+1/3}-u'^{n+1/2}_{j-2/3,k+1/3})/6 \tag{2.18}$$

and

$$(u_\eta'^+)_{j,k}^{n+1/2}=(u'^{n+1/2}_{j+1/3,k+1/3}-u'^{n+1/2}_{j+1/3,k-2/3})/6 \tag{2.19}$$

where $u'^{n+1/2}_{j+1/3,k+1/3}$, $u'^{n+1/2}_{j-2/3,k+1/3}$, and $u'^{n+1/2}_{j+1/3,k-2/3}$ can be computed using

$$u'^{n+1/2}_{j,k}=\left(u+\frac{\Delta t}{2}u_t\right)^n_{j,k} \tag{2.20}$$

Then the first marching step of the a-ϵ scheme can be expressed by (2.12) and

$$(u_\zeta^+)_{j,k}^{n+1/2} = (u_\zeta'^+)_{j,k}^{n+1/2}+(\epsilon-1/2)(du_\zeta^+)_{j,k}^{n+1/2} \tag{2.21}$$

$$(u_\eta^+)_{j,k}^{n+1/2} = (u_\eta'^+)_{j,k}^{n+1/2}+(\epsilon-1/2)(du_\eta^+)_{j,k}^{n+1/2} \tag{2.22}$$

where $0\le\epsilon\le 1$, which is a parameter for controling the numerical diffusion, and

$$(du_\zeta^+)_{j,k}^{n+1/2}=2\left[(u_\zeta'^+)_{j,k}^{n+1/2}-(u_\zeta^{\circ+})_{j,k}^{n+1/2}\right] \tag{2.23}$$

$$(du_\eta^+)_{j,k}^{n+1/2}=2\left[(u_\eta'^+)_{j,k}^{n+1/2}-(u_\eta^{\circ+})_{j,k}^{n+1/2}\right] \tag{2.24}$$

For any $(j,k,n+1)\in\Omega_2$, the counterparts to (2.18) and (2.19) are

$$(u_\zeta'^+)_{j,k}^{n+1}=(u'^{n+1}_{j+2/3,k-1/3}-u'^{n+1}_{j-1/3,k-1/3})/6 \tag{2.25}$$

and

$$(u_\eta'^+)_{j,k}^{n+1}=(u'^{n+1}_{j-1/3,k+2/3}-u'^{n+1}_{j-1/3,k-1/3})/6 \tag{2.26}$$

where $u'^{n+1}_{j-1/3,k-1/3}$, $u'^{n+1}_{j+2/3,k-1/3}$, and $u'^{n+1}_{j-1/3,k+2/3}$ can be obtained by using

$$u'^{n+1}_{j,k}=\left(u+\frac{\Delta t}{2}u_t\right)^{n+1/2}_{j,k} \tag{2.27}$$

Then the second marching step in the a-ϵ scheme is formed by (2.15) and

$$(u_\zeta^+)_{j,k}^{n+1} = (u_\zeta'^+)_{j,k}^{n+1}+(\epsilon-1/2)(du_\zeta^+)_{j,k}^{n+1} \tag{2.28}$$

$$(u_\eta^+)_{j,k}^{n+1} = (u_\eta'^+)_{j,k}^{n+1}+(\epsilon-1/2)(du_\eta^+)_{j,k}^{n+1} \tag{2.29}$$

where

$$(du_\zeta^+)_{j,k}^{n+1} = 2\left[(u_\zeta'^+)_{j,k}^{n+1} - (u_\zeta^{\circ+})_{j,k}^{n+1}\right] \tag{2.30}$$

$$(du_\eta^+)_{j,k}^{n+1} = 2\left[(u_\eta'^+)_{j,k}^{n+1} - (u_\eta^{\circ+})_{j,k}^{n+1}\right] \tag{2.31}$$

Next, the weighted-average counterparts to $(u_\zeta'^+)_{j,k}^n$ and $(u_\eta'^+)_{j,k}^n$ in the a-ϵ scheme are introduced. As a preliminary, for $(j,k,n+1/2) \in \Omega_1$, let

$$x_1 = u'^{n+1/2}_{j+1/3,k+1/3} - u^{n+1/2}_{j,k} \tag{2.32}$$

$$x_2 = u'^{n+1/2}_{j-2/3,k+1/3} - u^{n+1/2}_{j,k} \tag{2.33}$$

$$x_3 = u'^{n+1/2}_{j+1/3,k-2/3} - u^{n+1/2}_{j,k} \tag{2.34}$$

and

$$(\theta_l)_{j,k}^{n+1/2} = \left[\sqrt{(u_x^{(l)})^2 + (u_y^{(l)})^2}\right]_{j,k}^{n+1/2}, \quad l = 1,2,3 \tag{2.35}$$

where

$$(u_x^{(1)})_{j,k}^{n+1/2} = -\frac{3}{2w}(x_2 + x_3) \qquad (u_y^{(1)})_{j,k}^{n+1/2} = \frac{(3b+w)x_2 + (3b-w)x_3}{2wh} \tag{2.36}$$

$$(u_x^{(2)})_{j,k}^{n+1/2} = \frac{3x_1}{2w} \qquad (u_y^{(2)})_{j,k}^{n+1/2} = -\frac{(3b+w)x_1 + 2wx_3}{2wh} \tag{2.37}$$

$$(u_x^{(3)})_{j,k}^{n+1/2} = \frac{3x_1}{2w} \qquad (u_y^{(3)})_{j,k}^{n+1/2} = \frac{(w-3b)x_1 + 2wx_2}{2wh} \tag{2.38}$$

For any $\alpha \geq 0$, the weighted-average counterparts to $u_\zeta'^+$ and $u_\eta'^+$ are

$$u_\zeta^{w+} = \begin{cases} 0, & \text{if } \theta_1 = \theta_2 = \theta_3 = 0 \\ \dfrac{(\theta_2\theta_3)^\alpha u_\zeta^{(1)+} + (\theta_3\theta_1)^\alpha u_\zeta^{(2)+} + (\theta_1\theta_2)^\alpha u_\zeta^{(3)+}}{(\theta_1\theta_2)^\alpha + (\theta_2\theta_3)^\alpha + (\theta_3\theta_1)^\alpha}, & \text{otherwise} \end{cases} \tag{2.39}$$

and

$$u_\eta^{w+} = \begin{cases} 0, & \text{if } \theta_1 = \theta_2 = \theta_3 = 0 \\ \dfrac{(\theta_2\theta_3)^\alpha u_\eta^{(1)+} + (\theta_3\theta_1)^\alpha u_\eta^{(2)+} + (\theta_1\theta_2)^\alpha u_\eta^{(3)+}}{(\theta_1\theta_2)^\alpha + (\theta_2\theta_3)^\alpha + (\theta_3\theta_1)^\alpha}, & \text{otherwise} \end{cases} \tag{2.40}$$

where

$$(u_\zeta^{(1)+})_{j,k}^{n+1/2} = -(2x_2 + x_3)/6 \qquad (u_\eta^{(1)+})_{j,k}^{n+1/2} = -(x_2 + 2x_3)/6 \tag{2.41}$$

$$(u_\zeta^{(2)+})_{j,k}^{n+1/2} = (2x_1 + x_3)/6 \qquad (u_\eta^{(2)+})_{j,k}^{n+1/2} = (x_1 - x_3)/6 \tag{2.42}$$

$$(u_\zeta^{(3)+})_{j,k}^{n+1/2} = (x_1 - x_2)/6 \qquad (u_\eta^{(3)+})_{j,k}^{n+1/2} = (2x_1 + x_2)/6 \tag{2.43}$$

For $(j, k, n+1) \in \Omega_2$, there are

$$y_1 = u'^{n+1}_{j-1/3,k-1/3} - u^{n+1}_{j,k} \tag{2.44}$$

$$y_2 = u'^{n+1}_{j+2/3,k-1/3} - u^{n+1}_{j,k} \tag{2.45}$$

$$y_3 = u'^{n+1}_{j-1/3,k+2/3} - u^{n+1}_{j,k} \tag{2.46}$$

The counterparts to (2.41)–(2.43) and (2.36)–(2.38) are, respectively,

$$(u_\zeta^{(1)+})_{j,k}^{n+1} = (2y_2 + y_3)/6 \qquad (u_\eta^{(1)+})_{j,k}^{n+1} = (y_2 + 2y_3)/6 \tag{2.47}$$

$$(u_\zeta^{(2)+})_{j,k}^{n+1} = -(2y_1 + y_3)/6 \qquad (u_\eta^{(2)+})_{j,k}^{n+1} = -(y_1 - y_3)/6 \tag{2.48}$$

$$(u_\zeta^{(3)+})_{j,k}^{n+1} = -(y_1 - y_2)/6 \qquad (u_\eta^{(3)+})_{j,k}^{n+1} = -(2y_1 + y_2)/6 \tag{2.49}$$

and

$$(u_x^{(1)})_{j,k}^{n+1} = \frac{3}{2w}(y_2 + y_3) \qquad (u_y^{(1)})_{j,k}^{n+1} = -\frac{(3b+w)y_2 + (3b-w)y_3}{2wh} \tag{2.50}$$

$$(u_x^{(2)})_{j,k}^{n+1} = -\frac{3y_1}{2w} \qquad (u_y^{(2)})_{j,k}^{n+1} = \frac{(3b+w)y_1 + 2wy_3}{2wh} \tag{2.51}$$

$$(u_x^{(3)})_{j,k}^{n+1} = -\frac{3y_1}{2w} \qquad (u_y^{(3)})_{j,k}^{n+1} = -\frac{(w-3b)y_1 + 2wy_2}{2wh} \tag{2.52}$$

Equation (2.35) is still valid after changing the index $(n+1/2)$ into $(n+1)$. With the above definitions, (2.39) and (2.40) can be used as the the weighted-average part for a mesh point $(j, k, n+1) \in \Omega_2$.

Finally, the weighted-average α-ϵ scheme is generalized. The first marching step is formed by (2.12),

$$(u_\zeta^+)_{j,k}^{n+1/2} = (u_\zeta^{w+})_{j,k}^{n+1/2} + (\epsilon - 1/2)(du_\zeta^+)_{j,k}^{n+1/2} \tag{2.53}$$

and

$$(u_\eta^+)_{j,k}^{n+1/2} = (u_\eta^{w+})_{j,k}^{n+1/2} + (\epsilon - 1/2)(du_\eta^+)_{j,k}^{n+1/2} \tag{2.54}$$

where $(j, k, n+1/2) \in \Omega_1$. The second marching step is formed by (2.15),

$$(u_\zeta^+)_{j,k}^{n+1} = (u_\zeta^{w+})_{j,k}^{n+1} + (\epsilon - 1/2)(du_\zeta^+)_{j,k}^{n+1} \tag{2.55}$$

and

$$(u_\eta^+)_{j,k}^{n+1} = (u_\eta^{w+})_{j,k}^{n+1} + (\epsilon - 1/2)(du_\eta^+)_{j,k}^{n+1} \tag{2.56}$$

where $(j,k,n+1) \in \Omega_2$.

The accuracy of the a-ϵ scheme is the same as that of the a-μ scheme. The stability condition is discussed in [3].

3. The μ Scheme for Unsteady Diffusion Equation

The unsteady diffusion equation is a typical parabolic second-order partial differential equation. It is a special form of Eq. (1.1) with $a_x = a_y = 0$,

$$\frac{\partial u}{\partial t} = \mu\left(\frac{\partial^2 u}{\partial x^2} + \frac{\partial^2 u}{\partial y^2}\right) \tag{3.1}$$

For the interior CEs, the μ scheme is a special form of the a-μ scheme by letting $\nu_\zeta = \nu_\eta = 0$. For the boundary CEs, the scheme depends on the boundary conditions. If one flow variable is unknown at the boundary mesh points, only one conservation relation is needed. Referred to Fig. 2, for the boundary mesh point $(j,k,n+1/2) \in \Omega_1$, Eqs. (1.35), (1.36) and (1.37) can be obtained on the boundary at $x = 0$ with $k = 2,4,6,\cdots,ny-1$, at $y = 0$ with $j = 1,3,5,\cdots,nx-1$, and at $y = 1$ with $j = 1,3,5,\cdots,nx-1$, respectively. For the boundary mesh point $(j,k,n+1) \in \Omega_2$, Eqs. (1.38), (1.40) and (1.39) can be obtained on the boundary mesh points at $x = 1$ with $k = 3,5,7,\cdots,ny-2$, at $y = 0$ with $j = 2,4,6,\cdots,nx-2$, and at $y = 1$ with $j = 2,4,6,\cdots,nx-2$, respectively.

It is assumed that the value of $(u_x)^n_{j,k}$ is unknown on the boundaries at $x = 0$ and $x = 1$ and the value of $(u_y)^n_{j,k}$ is unknown on the boundaries at $y = 0$ and $y = 1$, respectively. And we know

$$(u^+_\zeta)^n_{j,k} = \left[(w-b)(u_x)^n_{j,k} - h(u_y)^n_{j,k}\right]/6 \tag{3.2}$$

$$(u^+_\eta)^n_{j,k} = \left[(w+b)(u_x)^n_{j,k} + h(u_y)^n_{j,k}\right]/6 \tag{3.3}$$

Substituting (3.2) and (3.3) into (1.35)–(1.40), one can obtain

$$(u_x)^n_{1,k} = \frac{6s^{(1)}_1 - 6\sigma^{(1)+}_{11}u^{n+1/2}_{1,k} + h\sigma^{(1)+}_{12}(u_y)^{n+1/2}_{1,k} - h\sigma^{(1)+}_{13}(u_y)^{n+1/2}_{1,k}}{\sigma^{(1)+}_{12}(w-b) + \sigma^{(1)+}_{13}(w+b)} \tag{3.4}$$

$$(u_y)^{n+1/2}_{j,1} = \frac{6s^{(1)}_2 - 6\sigma^{(1)+}_{21}u^{n+1/2}_{j,1} - (w-b)\sigma^{(1)+}_{22}(u_x)^{n+1/2}_{j,1} - (w+b)\sigma^{(1)+}_{23}(u_x)^{n+1/2}_{j,1}}{h(-\sigma^{(1)+}_{22} + \sigma^{(1)+}_{23})} \tag{3.5}$$

$$(u_y)^{n+1/2}_{j,ny} = \frac{6s^{(1)}_3 - 6\sigma^{(1)+}_{31}u^{n+1/2}_{j,ny} - (w-b)\sigma^{(1)+}_{32}(u_x)^{n+1/2}_{j,ny} - (w+b)\sigma^{(1)+}_{33}(u_x)^{n+1/2}_{j,ny}}{h(-\sigma^{(1)+}_{32} + \sigma^{(1)+}_{33})} \tag{3.6}$$

for the boundary mesh points $(j,k,n+1/2)\in\Omega_1$, and

$$(u_x)^{n+1}_{nx,k}=\frac{6s^{(2)}_1-6\sigma^{(2)+}_{11}u^{n+1}_{nx,k}+h\sigma^{(2)+}_{12}(u_y)^{n+1}_{nx,k}-h\sigma^{(2)+}_{13}(u_y)^{n+1}_{nx,k}}{\sigma^{(2)+}_{12}(w-b)+\sigma^{(2)+}_{13}(w+b)}, \tag{3.7}$$

$$(u_y)^{n+1}_{j,1}=\frac{6s^{(2)}_3-6\sigma^{(2)+}_{31}u^{n+1}_{j,1}-(w-b)\sigma^{(2)+}_{32}(u_x)^{n+1}_{j,1}-(w+b)\sigma^{(2)+}_{33}(u_x)^{n+1}_{j,1}}{h(-\sigma^{(2)+}_{32}+\sigma^{(2)+}_{33})} \tag{3.8}$$

$$(u_y)^{n+1}_{j,ny}=\frac{6s^{(2)}_2-6\sigma^{(2)+}_{21}u^{n+1}_{j,ny}-(w-b)\sigma^{(2)+}_{22}(u_x)^{n+1}_{j,ny}-(w+b)\sigma^{(2)+}_{23}(u_x)^{n+1}_{j,ny}}{h(-\sigma^{(2)+}_{22}+\sigma^{(2)+}_{23})} \tag{3.9}$$

for the boundary mesh points $(j,k,n+1)\in\Omega_2$.

Equations (3.4)–(3.9) are the μ scheme for the boundary mesh points. Once $(u_x)^n_{j,k}$ and $(u_y)^n_{j,k}$ become known, $(u_\zeta)^n_{j,k}$ and $(u_\eta)^n_{j,k}$ can be obtained using (3.2) and (3.3). Note that $\nu_\zeta=\nu_\eta=0$ in $\sigma^{(1)+}_{11},\sigma^{(1)+}_{12},\cdots$ and $s^1_1,s^{(1)}_2,\cdots$ in (3.4)–(3.9). The μ scheme is characterized only by the diffusion numbers $\xi_\zeta,\xi_\eta,\xi_\tau$ and is unconditionally stable with the same accuracy as the a-μ scheme.

4. The ν-ϵ Scheme for Inviscid Burgers Equation

The inviscid Burgers equation in conservative form is

$$\frac{\partial u}{\partial t}+\frac{\partial f}{\partial x}+\frac{\partial f}{\partial y}=0 \tag{4.1}$$

where $f=0.5u^2$. Its integral form in the space-time E_3 is the same as (1.3), except $\vec{h}=(f,f,u)$ here. Some additional definitions cooresponding to f are

$$f^u=\partial f/\partial u=u,\quad f=0.5f^uu \tag{4.2}$$

$$f_x=\partial f/\partial x=f^uu_x,\quad f_y=\partial f/\partial y=f^uu_y,\quad f_t=\partial f/\partial t=f^uu_t \tag{4.3}$$

Similarly, $f(x,y,t;j,k,n)$ is approximated by

$$f^*(x,y,t;j,k,n)=f^n_{j,k}+(f_x)^n_{j,k}(x-x_{j,k})+(f_y)^n_{j,k}(y-y_{j,k})+(f_t)^n_{j,k}(t-t^n) \tag{4.4}$$

thus

$$\vec{h}^*(x,y,t;j,k,n)=(f^*(x,y,t;j,k,n),f^*(x,y,t;j,k,n),u^*(x,y,t;j,k,n)) \tag{4.5}$$

Note that $(f_x)^n_{j,k},(f_y)^n_{j,k}$, and $(f_t)^n_{j,k}$ are functions of $(u)^n_{j,k},(u_x)^n_{j,k},(u_y)^n_{j,k}$, and $(u_t)^n_{j,k}$. From the assumption of

$$\frac{\partial u^*(x,y,t;j,k,n)}{\partial t}+\frac{\partial f^*(x,y,t;j,k,n)}{\partial x}+\frac{\partial f^*(x,y,t;j,k,n)}{\partial y}=0 \tag{4.6}$$

one obtains

$$u_t = -f_x - f_y = -(f^u u_x + f^u u_y) \tag{4.7}$$

One can conclude that there are also three independent variables, namely $(u)^n_{j,k}, (u_x)^n_{j,k}$, and $(u_y)^n_{j,k}$, associated with each mesh point $(j,k,n) \in \Omega$.

Furthermore, the corresponding coefficients in the (ζ,η) coordinate are

$$\begin{pmatrix} f^\zeta \\ f^\eta \end{pmatrix} = T^{-1} \begin{pmatrix} f^u \\ f^u \end{pmatrix}, \quad \begin{pmatrix} f^{\zeta+} \\ f^{\eta+} \end{pmatrix} = \frac{3}{2}\Delta t \begin{pmatrix} f^\zeta/\Delta\zeta \\ f^\eta/\Delta\eta \end{pmatrix} \tag{4.8}$$

Then the counterparts to (1.17)–(1.34) are:

$$\bar{\sigma}^{(1)\pm}_{11} = 1 - 0.5f^{\zeta+} - 0.5f^{\eta+} \tag{4.9}$$
$$\bar{\sigma}^{(1)\pm}_{12} = \pm(1 - f^{\zeta+} - f^{\eta+})(1 + f^{\zeta+}) \tag{4.10}$$
$$\bar{\sigma}^{(1)\pm}_{13} = \pm(1 - f^{\zeta+} - f^{\eta+})(1 + f^{\eta+}) \tag{4.11}$$
$$\bar{\sigma}^{(1)\pm}_{21} = 1 + 0.5f^{\zeta+} \tag{4.12}$$
$$\bar{\sigma}^{(1)\pm}_{22} = \mp(1 + f^{\zeta+})(2 - f^{\zeta+}) \tag{4.13}$$
$$\bar{\sigma}^{(1)\pm}_{23} = \pm(1 + f^{\zeta+})(1 + f^{\eta+}) \tag{4.14}$$
$$\bar{\sigma}^{(1)\pm}_{31} = 1 + 0.5f^{\eta+} \tag{4.15}$$
$$\bar{\sigma}^{(1)\pm}_{32} = \pm(1 + f^{\eta+})(1 + f^{\zeta+}) \tag{4.16}$$
$$\bar{\sigma}^{(1)\pm}_{33} = \mp(1 + f^{\eta})(2 - f^{\eta+}) \tag{4.17}$$
$$\bar{\sigma}^{(2)\pm}_{11} = 1 + 0.5f^{\zeta+} + 0.5f^{\eta+} \tag{4.18}$$
$$\bar{\sigma}^{(2)\pm}_{12} = \mp(1 + f^{\zeta+} + f^{\eta+})(1 - f^{\zeta+}) \tag{4.19}$$
$$\bar{\sigma}^{(2)\pm}_{13} = \mp(1 + f^{\zeta+} + f^{\eta+})(1 - f^{\eta+}) \tag{4.20}$$
$$\bar{\sigma}^{(2)\pm}_{21} = 1 - 0.5f^{\zeta+} \tag{4.21}$$
$$\bar{\sigma}^{(2)\pm}_{22} = \pm(1 - f^{\zeta+})(2 + f^{\zeta+}) \tag{4.22}$$
$$\bar{\sigma}^{(2)\pm}_{23} = \mp(1 - f^{\zeta+})(1 - f^{\eta+}) \tag{4.23}$$
$$\bar{\sigma}^{(2)\pm}_{31} = 1 - 0.5f^{\eta+} \tag{4.24}$$
$$\bar{\sigma}^{(2)\pm}_{32} = \mp(1 - f^{\eta+})(1 - f^{\zeta+}) \tag{4.25}$$
$$\bar{\sigma}^{(2)\pm}_{33} = \pm(1 - f^{\eta+})(2 + f^{\eta+}) \tag{4.26}$$

Let $\bar{s}^{(1)}_1, \bar{s}^{(1)}_2, \bar{s}^{(1)}_3, \bar{s}^{(2)}_1, \bar{s}^{(2)}_2$, and $\bar{s}^{(2)}_3$ denote the expressions on the right sides of (1.35)–(1.40), in which $\sigma^{(1)+}_{11}, \sigma^{(1)-}_{11}, \cdots$ are replaced by $\bar{\sigma}^{(1)+}_{11}, \bar{\sigma}^{(1)-}_{11}, \cdots$. From (1.35)–(1.37) and

(1.38)–(1.40), respectively, one obtains

$$u_{j,k}^{n+1/2} = \frac{1}{3}\left[\bar{s}_1^{(1)} + \bar{s}_2^{(1)} + \bar{s}_3^{(1)}\right] \tag{4.27}$$

$$\begin{aligned}(u_\zeta^{\circ+})_{j,k}^{n+1/2} = \frac{1}{3}\Big\{&\left[\bar{s}_1^{(1)} - (\bar{\sigma}_{11}^{(1)+}u)_{j,k}^{n+1/2}\right]/(2\bar{\sigma}_{11}^{(1)+} - 1)_{j,k}^{n+1/2} \\ &- \left[\bar{s}_2^{(1)} - (\bar{\sigma}_{21}^{(1)+}u)_{j,k}^{n+1/2}\right]/(2\bar{\sigma}_{21}^{(1)+} - 1)_{j,k}^{n+1/2}\Big\}\end{aligned} \tag{4.28}$$

$$\begin{aligned}(u_\eta^{\circ+})_{j,k}^{n+1/2} = \frac{1}{3}\Big\{&\left[\bar{s}_1^{(1)} - (\bar{\sigma}_{11}^{(1)+}u)_{j,k}^{n+1/2}\right]/(2\bar{\sigma}_{11}^{(1)+} - 1)_{j,k}^{n+1/2} \\ &- \left[\bar{s}_3^{(1)} - (\bar{\sigma}_{31}^{(1)+}u)_{j,k}^{n+1/2}\right]/(2\bar{\sigma}_{31}^{(1)+} - 1)_{j,k}^{n+1/2}\Big\}\end{aligned} \tag{4.29}$$

for any $(j,k,n+1/2) \in \Omega_1$, and

$$u_{j,k}^{n+1} = \frac{1}{3}\left[\bar{s}_1^{(2)} + \bar{s}_2^{(2)} + \bar{s}_3^{(2)}\right] \tag{4.30}$$

$$\begin{aligned}(u_\zeta^{\circ+})_{j,k}^{n+1} = \frac{1}{3}\Big\{&\left[\bar{s}_2^{(2)} - (\bar{\sigma}_{21}^{(2)+}u)_{j,k}^{n+1}\right]/(2\bar{\sigma}_{21}^{(2)+} - 1)_{j,k}^{n+1} \\ &- \left[\bar{s}_1^{(2)} - (\bar{\sigma}_{11}^{(2)+}u)_{j,k}^{n+1}\right]/(2\bar{\sigma}_{11}^{(2)+} - 1)_{j,k}^{n+1}\Big\}\end{aligned} \tag{4.31}$$

$$\begin{aligned}(u_\eta^{\circ+})_{j,k}^{n+1} = \frac{1}{3}\Big\{&\left[\bar{s}_3^{(2)} - (\bar{\sigma}_{31}^{(2)+}u)_{j,k}^{n+1}\right]/(2\bar{\sigma}_{31}^{(2)+} - 1)_{j,k}^{n+1} \\ &- \left[\bar{s}_1^{(2)} - (\bar{\sigma}_{11}^{(2)+}u)_{j,k}^{n+1}\right]/(2\bar{\sigma}_{11}^{(2)+} - 1)_{j,k}^{n+1}\Big\}\end{aligned} \tag{4.32}$$

for any $(j,k,n+1) \in \Omega_2$.

Equations (2.18)–(2.56) are valid in the weighted-average ν-ϵ scheme. The accuracy of ν-ϵ scheme is also second-order in time and space. The stability condition is the same as that of a-ϵ scheme with ν_ζ and ν_η replaced by $f^{\zeta+}$ and $f^{\eta+}$ which are not constants any more.

Test Problems and Discussions

All of the two-dimensional schemes described in the previous section are tested using standard model problems. The numerical results are compared with either the exact solutions or the numerical solutions obtained by some traditional finite-difference or finite-element methods to examine their accuracy, simplicity and effectiveness.

1. Test of the a-μ Scheme

The translating Gaussian hill problem that was solved by using Taylor-Galerkin finite-element method in [5] is investigated here again. The governing equation is

$$\frac{\partial u}{\partial t} + a_x \frac{\partial u}{\partial x} + a_y \frac{\partial u}{\partial y} = \mu\left(\frac{\partial^2 u}{\partial x^2} + \frac{\partial^2 u}{\partial y^2}\right), \quad -1 \le x \le 1, -1 \le y \le 1$$

which describes the problem that a Gaussian hill translates with a uniform velocity $\vec{a} = (a_x, a_y)$ and spreads isotropically with a diffusivity μ. Its exact solution is

$$u(x,y,t) = \frac{1}{\sigma^2(t)} \exp\left[-\frac{1}{2\sigma^2(t)}\left((x - x_0 - a_x t)^2 + (y - y_0 - a_y t)^2\right)\right]$$

where $\sigma(t) = \sigma_0\sqrt{1 + 2\mu t/\sigma_0^2}$, $a_x = a\cos\phi$, $a_y = a\sin\phi$, in which ϕ is the angle between the advection velocity and the x axis. In this problem, the initial conditions

$$\begin{aligned} u(x,y,0) &= \frac{1}{\sigma_0^2} \exp\left[-\frac{1}{2\sigma_0^2}\left((x - x_0)^2 + (y - y_0)^2\right)\right] \\ u_x(x,y,0) &= -\frac{u(x,y,0)}{\sigma_0^2}(x - x_0) \\ u_y(x,y,0) &= -\frac{u(x,y,0)}{\sigma_0^2}(y - y_0) \end{aligned}$$

are set as the exact solution at t=0, where $\sigma_0 = 0.0707$, $\phi = 45°$, $x_0 = y_0 = -0.5$ are used.

The grid size used in the a-μ scheme is initially 25×86. Figure 3 shows the numerical solution and the distribution of the absolute error, which is defined as $|u^n_{j,k} - u_e|$, for $\mu = 0.0125$ at t=0.5. The relative L_2 error, which is defined as

$$L_2 = \frac{\sqrt{\sum_{i,j=1}^{n-1,m-1}(u_e - u^n_{i,j})^2/(n-1)(m-1)}}{u_{max}}$$

obtained with $\Delta t = 0.02$ is 6.997×10^{-4} and the numerical maximum value is 99.21% of the corresponding exact value. When the grid size is doubled to 50×173 and with $\Delta t = 0.005$, the relative L_2 error is reduced to 3.84×10^{-5} and the numerical maximum value becomes 99.97% of the exact value.

The same problem is then solved but with a much higher diffusivity of $\mu = 0.0625$. Figure 4 shows the numerical solution and the absolute error distribution at t=0.5. The relative L_2 error of the numerical solution obtained on a 25×86 grid with $\Delta t = 0.02$ is 1.788×10^{-2} and the numerical maximum value is 96.07% of the exact value. Similiarly,

the relative L_2 error can be improved to 3.363×10^{-3} and the numerical maximum value is up to 98.68% of the exact value by doubling the grid size to 50×173 with $\Delta t = 0.005$.

Numerical results of the a-μ scheme depict that its accuracy can be improved by using finer grid meshes and it can generate more accurate numerical solutions for lower diffusivities. Once the grid size is fixed, the time step size will be the only parameter to determine the accuracy and stability. In the first test case with $\mu = 0.0125$, different time step sizes have been used to obtain the best results as well as to satisfy the stability condition. In the second test case with $\nu = 0.0625$, the same time step sizes as those in the first case are used for a fair comparison between the numerical solutions for lower and higher diffusivity. The comparisons show that the numerical solutions for the lower diffusivity is more accurate.

2. Test of the a-ϵ Scheme

The a-ϵ scheme expressed in (2.12), (2.21), (2.22) and (2.15), (2.28), (2.29) is used to solve the problem that a Gaussian hill travels with a uniform advection velocity $\vec{a} = (a_x, a_y)$ without diffusivity, which is a special case of the previous Gaussian hill test problem. The governing equation is the pure advection equation

$$\frac{\partial u}{\partial t} + a_x \frac{\partial u}{\partial x} + a_y \frac{\partial u}{\partial y} = 0, \quad -1 \le x \le 1, \quad -1 \le y \le 1$$

The exact solution and initial conditions are the same as those in the previous problem by letting $\mu = 0$. The exact solution is shown in Fig. 5(a). Numerical solutions at t=1.0 obtained by using the same time step size $\Delta t = 0.02$ on a 50×173 grid are shown in Figs. 5(b)–5(d) for $\epsilon = 0$, 0.1, and 0.3, respectively. There are some oscillations along the direction of advection velocity when $\epsilon = 0$; they disappear when $\epsilon = 0.1$ or 0.3. But the relative L_2 error are 4.514×10^{-3}, 2.83×10^{-3}, and 3.08×10^{-3}, and the numerical maximum values are 98.2%, 97.6%, and 97.4% of the exact value for $\epsilon = 0$, 0.1, and 0.3, respectively. It can be seen that the numerical oscillation can be suppressed by increasing ϵ and, meanwhile, the maximum value deviates more from the exact value because of the increased numerical diffusion. A large ϵ may lead to too much numerical diffusion which is not expected. The solution with $\epsilon = 0.1$ is the best for this problem.

3. Test of the μ Scheme

The μ scheme is used to solve the unsteady diffusion equation

$$\frac{\partial u}{\partial t} = \mu\left(\frac{\partial^2 u}{\partial x^2} + \frac{\partial^2 u}{\partial y^2}\right), \quad 0 \le x \le 1, \quad 0 \le y \le 1$$

which was solved in [6, pp.259-266] by using Crank-Nicolson implicit finite-difference and finite-element methods.

The initial conditions are stated as follows:

$$\begin{aligned} u(x,y,0) &= 20 + 80\,[y - \sin(0.5\pi x)\sin(0.5\pi y)] \\ u_x(x,y,0) &= -40\pi\cos(0.5\pi x)\sin(0.5\pi y) \\ u_y(x,y,0) &= 80 - 40\pi\sin(0.5\pi x)\cos(0.5\pi y) \end{aligned}$$

which are defined by the exact solution

$$u(x,y,t) = 20 + 80\left[y - e^{-0.5\mu\pi^2 t}\sin(0.5\pi x)\sin(0.5\pi y)\right]$$

at t=0. The boundary conditions are:

$$\begin{aligned} u(0,y,t) &= 20 + 80y \\ u(1,y,t) &= 20 + 80\left[y - e^{-0.5\mu\pi^2 t}\sin(0.5\pi y)\right] \\ u(x,0,t) &= 20 \\ u(x,1,t) &= 20 + 80\left[1 - e^{-0.5\mu\pi^2 t}\sin(0.5\pi x)\right] \end{aligned}$$

and

$$\begin{aligned} u_y(0,y,t) &= 80 \\ u_y(1,y,t) &= 80\left[1 - 0.5\pi e^{-0.5\mu\pi^2 t}\cos(0.5\pi y)\right] \\ u_x(x,0,t) &= 0 \\ u_x(x,1,t) &= -40\pi e^{-0.5\mu\pi^2 t}\cos(0.5\pi x) \end{aligned}$$

Equations (3.4)–(3.9) are used at the boundary CEs.

A 6×21 grid is used here for computation. Figure 6 shows the numerical solution at t=24000. The L_2 error is defined as

$$L_2 = \sqrt{\frac{\sum_{i,j=1}^{n-1,m-1}(u_e - u_{i,j}^n)^2}{(n-1)\times(m-1)}}$$

which is the same as that in [6]. The L_2 error is 5.9889×10^{-4} obtained by the μ scheme with $\Delta t = 100$. Considering the results obtained by all of the numerical methods mentioned in [6] having the same accuracy $(\Delta t, (\Delta x)^2, (\Delta y)^2)$ as the μ scheme, the best one is the Crank-Nicolson implicit finite-element method, whose errors are respectively $L_2 = 6.86\times10^{-3}$ with

a 10×10 grid, and 1.59×10^{-3} with a 20×20 grid. The numerical results can be improved so that those errors are reduced to 1.34×10^{-4} and 8.2×10^{-5}, respectively, by using the higher-order Crank-Nicolson method which has the $((\Delta t)^2, (\Delta x)^4, (\Delta y)^4)$ truncation error. By using the μ scheme with more grid points, such as 30×60, an improvement is obtained having $L_2 = 1.3467 \times 10^{-4}$ with $\Delta t = 12$. However, additional improvements cannot be achieved by further refinement of the grid, showing the need of a higher order accurate implicit scheme based on the CE/SE method.

4. Test of the ν-ϵ Scheme

Consider the inviscid Burgers equation

$$\frac{\partial u}{\partial t} + \frac{\partial f}{\partial x} + \frac{\partial f}{\partial y} = 0, \quad 0 \le x \le 1, \quad 0 \le y \le 1.$$

where $f = \frac{1}{2}u^2$, that has a discontinuous initial condition described by

$$\begin{aligned} u(x,y,0) &= \frac{1}{2} && \text{if } x \le \frac{1}{2} \quad \text{and} \quad y \le \frac{1}{2} \\ &= -\frac{1}{2} && \text{if } x > \frac{1}{2} \quad \text{and} \quad y > \frac{1}{2} \\ &= \frac{1}{4} && \text{otherwise} \end{aligned}$$

for the first case, and

$$\begin{aligned} u(x,y,0) &= \frac{1}{2} && \text{if } x \le \frac{1}{2} \quad \text{and} \quad y \le \frac{1}{2} \\ &= \frac{1}{8} && \text{if } x > \frac{1}{2} \quad \text{and} \quad y > \frac{1}{2} \\ &= \frac{1}{4} && \text{otherwise} \end{aligned}$$

for the second case.

This problem contains complicated shock interaction, whose exact solution is referred to [7]. MacCormack's scheme is used to solve the same problem to test the techniques of using a moving finer mesh which follows the shock as described in [7], where the fine grid point is up to 100×100, and the boundary conditions are specified as the exact solution for the first case, whereas for the second case, the conditions at the inflow boundaries at $x = 0$ and $y = 0$ are specified as the exact solution, but those at the outflow boundaries at $x = 1$ and $y = 1$ are computed by interpolation from the upstream grid points. For

the first case at $t = 1.125$, the exact solution is plotted in Fig. 7(a) and the numerical solutions obtained by the weighted-average ν-ϵ scheme with grid sizes of 50×173 and 25×87 are shown in Figs. 7(b) and 7(c), respectively. Figures 8(a)–8(d) show the exact and numerical results for the second case at $t = 1.125$. In comparison with the numerical results by MacCormack's scheme shown in Figs. 2 and 5 of [7], the present results in both cases are much better except a little smear near one of the discontinuities, yet the scheme is so simple and no additional ad hoc techniques are needed. Even with the coarse 25×87 grid, the result is already much better. For a larger α, the numerical diffusion is larger and the smear near the discontinuity is more serious as depicted in Figs. 8(b) and 8(c).

Conclusion

The two-dimensional a-μ and a-ϵ schemes based on the space-time conservation element and solution element method have been used to solve the unsteady advection-diffusion equation, unsteady pure advection equation, and unsteady diffusion equation. The a-ϵ scheme has been modified to become the ν-ϵ scheme for solving the inviscid Burgers equation. Six numerical tests have been used to demonstrate that all of those schemes are superior to some of the traditional methods in accuracy and simplicity. The schemes themselves are physically sound, natural and simple. Highly accurate solutions can thus be obtained without using any ad hoc techniques. For further investigations, a more efficient implicit scheme with a higher accuracy based on the CE/SE method for solving the unsteady diffusion equation will be developed.

Acknowledgment

This work was supported by NASA Lewis Research Center through Grant NAG3-1566.

References

[1]. Chang, S.C., "New Developments in the Method of Space-Time Conservation Element and Solution Element—Applications to the Euler and Navier-Stokes Equations," NASA TM 106226, August, 1993.

[2]. Chang, S.C. and To, W.M., "A New Numerical Framework for Solving Conservation Laws—The Method of Space-Time Conservation Element and Solution Element," NASA TM 104495, August, 1991.

[3]. Chang, S.C., Wang, X.Y., and Chow, C.Y., "New Developments in the Method of Space-Time Conservation Element and Solution Element to Multi-dimensional Problems," to be published as NASA TM.

[4]. Wang, X.Y., Chow, C.Y., and Chang, S.C., "Application of the Space-Time Conservation Element and Solution Element Method to Two-dimensional Advection-Diffusion Problems," NASA TM .

[5]. Donea, J., Giuliani, S. and Laval, H., "Time-Accurate Solution of Advection-Diffusion Problems by Finite Elements," Computer Methods in Applied Mechanics and Engineering 45 (1984) 123–145, North-Holland.

[6]. Fletcher, C.A.J., *Computational Techniques for Fluid Dynamics 1*, 2nd edition, Springer-Verlag, Berlin, 1991.

[7]. Gropp, W.D., "A Test of Moving Mesh Refinement for 2-D Scalar Hyperbolic Problems," SIAM Journal of Scientific Statistical Computing, Vol. 1, No.2, June, 1980.

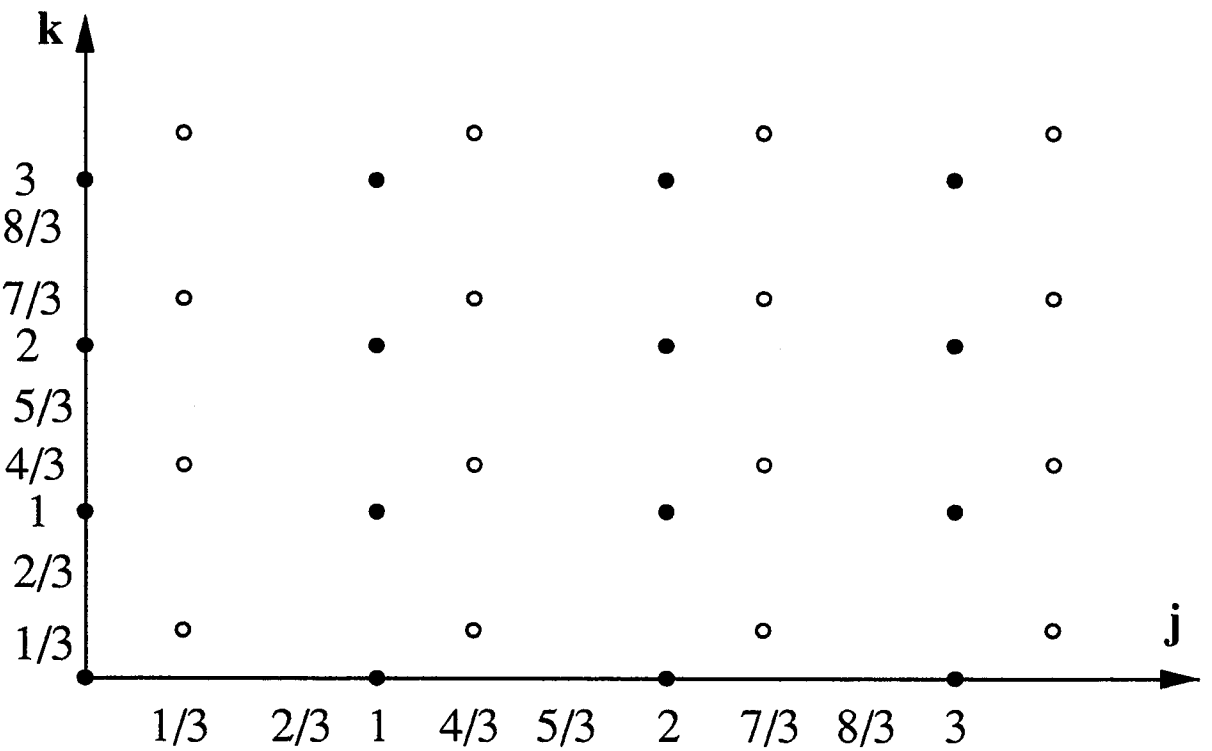

- at time levels n=0, 1, 2, 3 ...
- at time levels n=1/2, 3/2, 5/2 ....

(a) Spatial positions of the mesh points marked by solid and harrow circles

Fig. 1 The 2-D SEs and CEs in the CE/SE method

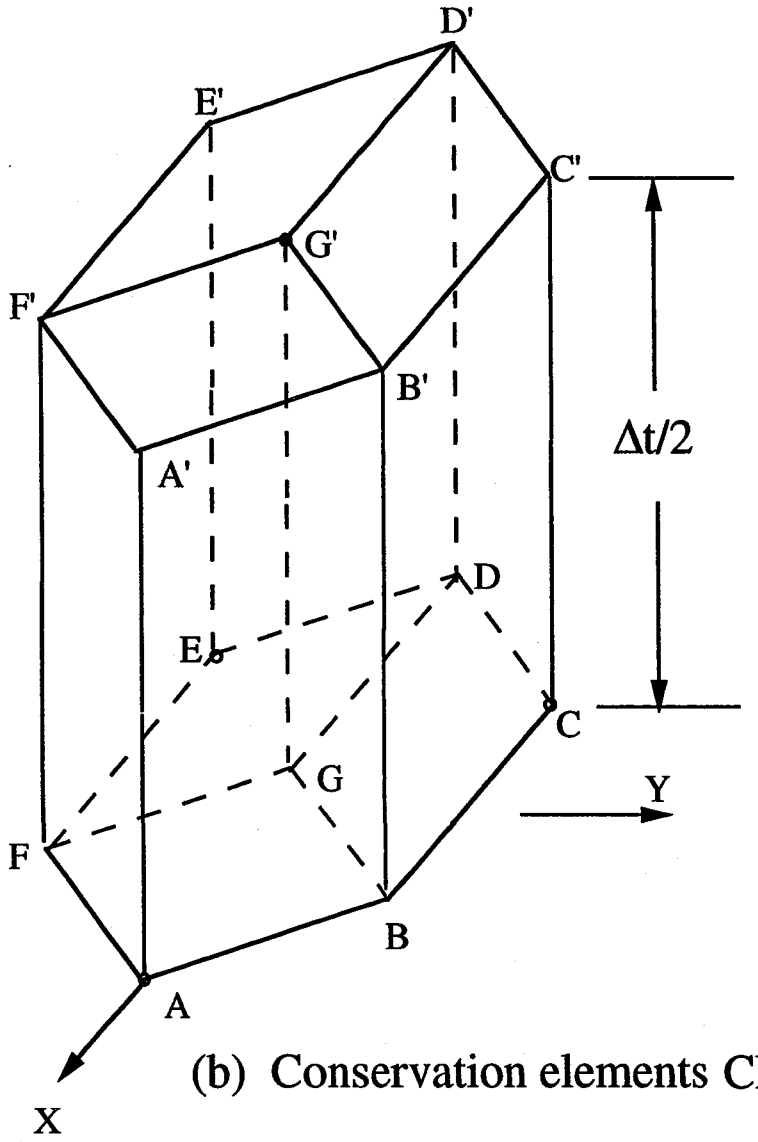

$G' = (j, k, n+1/2)$

$A = (j+1/3, k+1/3, n)$

$C = (j-2/3, k+1/3, n)$

$E = (j+1/3, k-2/3, n)$

$CE_1^{(1)}(j, k, n+1/2)$=box ABGFA'B'G'F'

$CE_2^{(1)}(j, k, n+1/2)$=box BCDGB'C'D'G'

$CE_3^{(1)}(j, k, n+1/2)$=box DEFGD'E'F'G'

(b) Conservation elements $CE_i^{(1)}(j, k, n+1/2)$, i=1, 2, 3, and j, k, n=0, ±1, ±2, ...

Fig. 1 Continued.

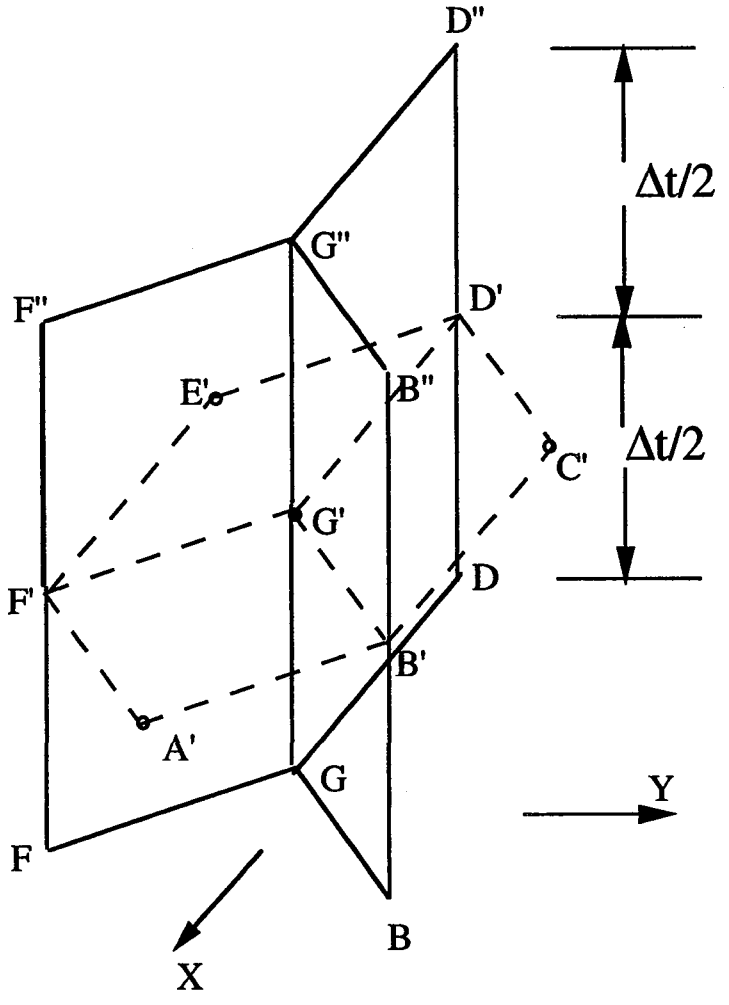

$G' = (j, k, n+1/2)$

$B' = (j-1/3, k+2/3, n+1/2)$

$D' = (j-1/3, k-1/3, n+1/2)$

$F' = (j+2/3, k-1/3, n+1/2)$

$SE^{(1)}(j, k, n+1/2)$ = The union of four planes A'B'C'D'E'F', GBB"G", GDD"G" and GG"F"F and their immediate neighborhoods.

(c) Solution element $SE^{(1)}(j, k, n+1/2)$, $j, k, n = 0, \pm1, \pm2, \ldots$

Fig. 1 Continued.

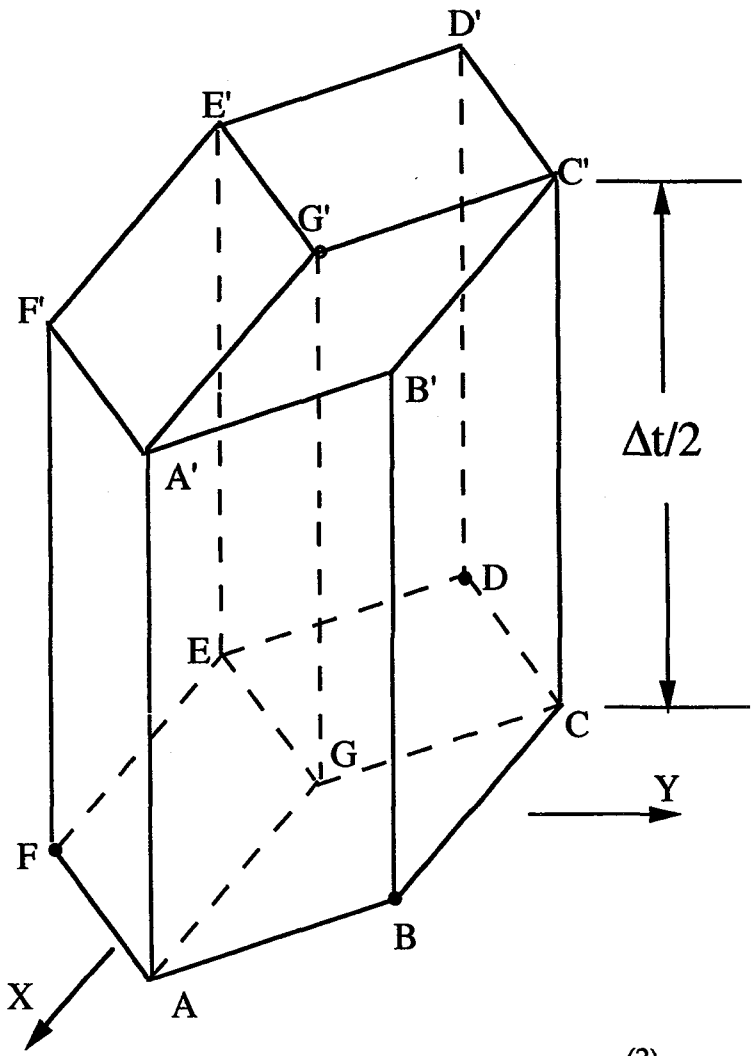

G' = (j, k, n+1)

B = (j-1/3, k+2/3, n+1/2)

D = (j-1/3, k-1/3, n+1/2)

F = (j+2/3, k-1/3, n+1/2)

$CE_1^{(2)}$(j, k, n+1)=box CDEGC'D'E'G'

$CE_2^{(2)}$(j, k, n+1)=box AGEFA'G'E'F'

$CE_3^{(2)}$(j, k, n+1)=box ABCGA'B'C'G'

(d) Conservation elements $CE_i^{(2)}$(j, k, n+1), i=1, 2, 3, and j, k=1/3, 1/3±1, 1/3±2, ..., and n=0, ±1, ±2,...

Fig. 1 Continued.

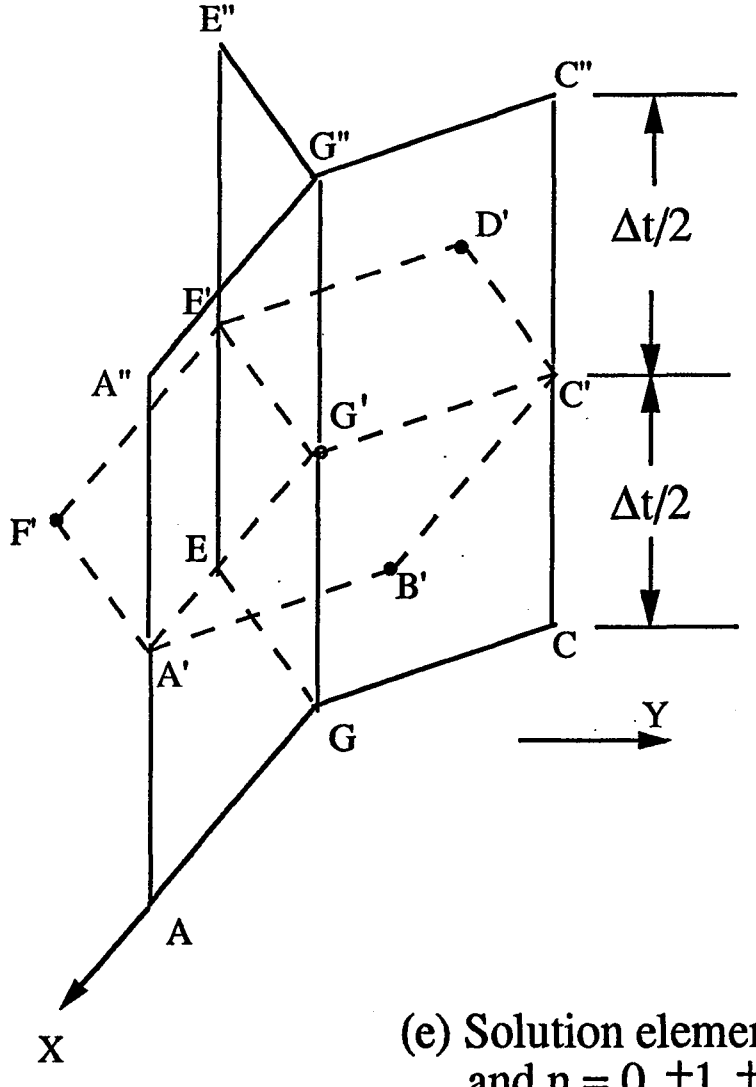

$G' = (j, k, n+1)$

$A' = (j+1/3, k+1/3, n+1)$

$C' = (j-2/3, k+1/3, n+1)$

$E' = (j+1/3, k-2/3, n+1)$

$SE^{(2)}(j, k, n+1)$ = The union of four planes A'B'C'D'E'F', GG"A"A, GCC"G" and GG"E"E and their immediate neighborhoods.

(e) Solution element $SE^{(2)}(j, k, n+1)$, $j, k = 1/3, 1/3 \pm 1, 1/3 \pm 2, \ldots$, and $n = 0, \pm 1, \pm 2, \ldots$

Fig. 1 Continued.

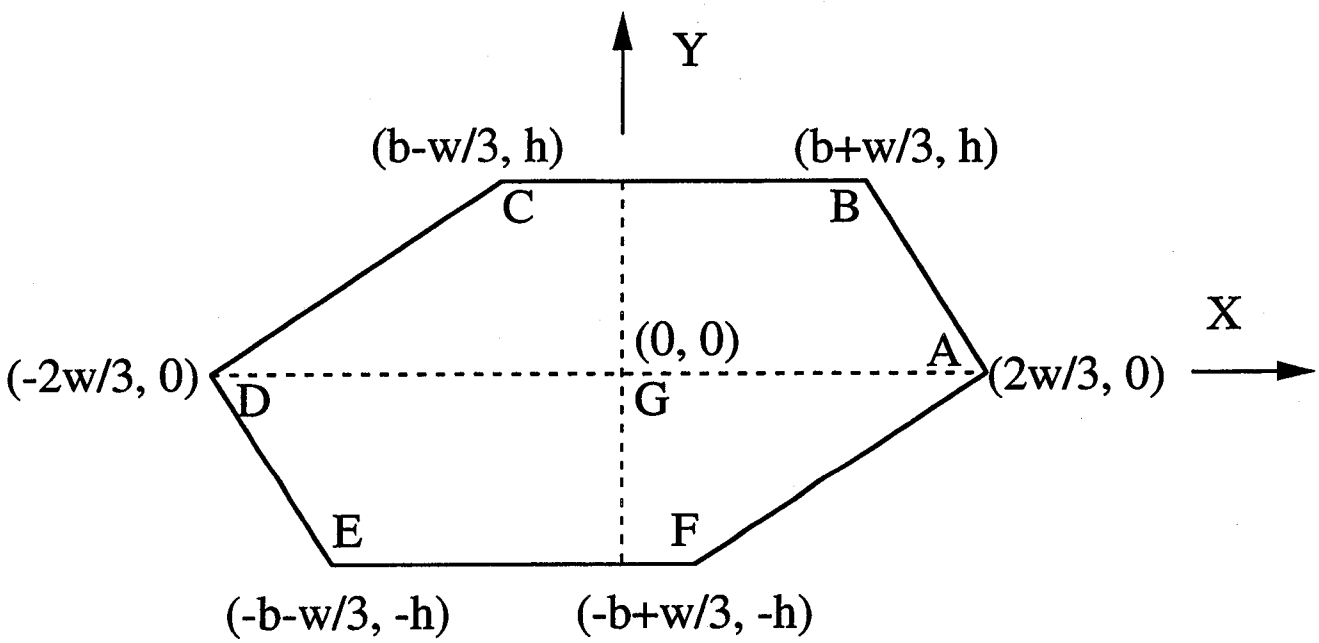

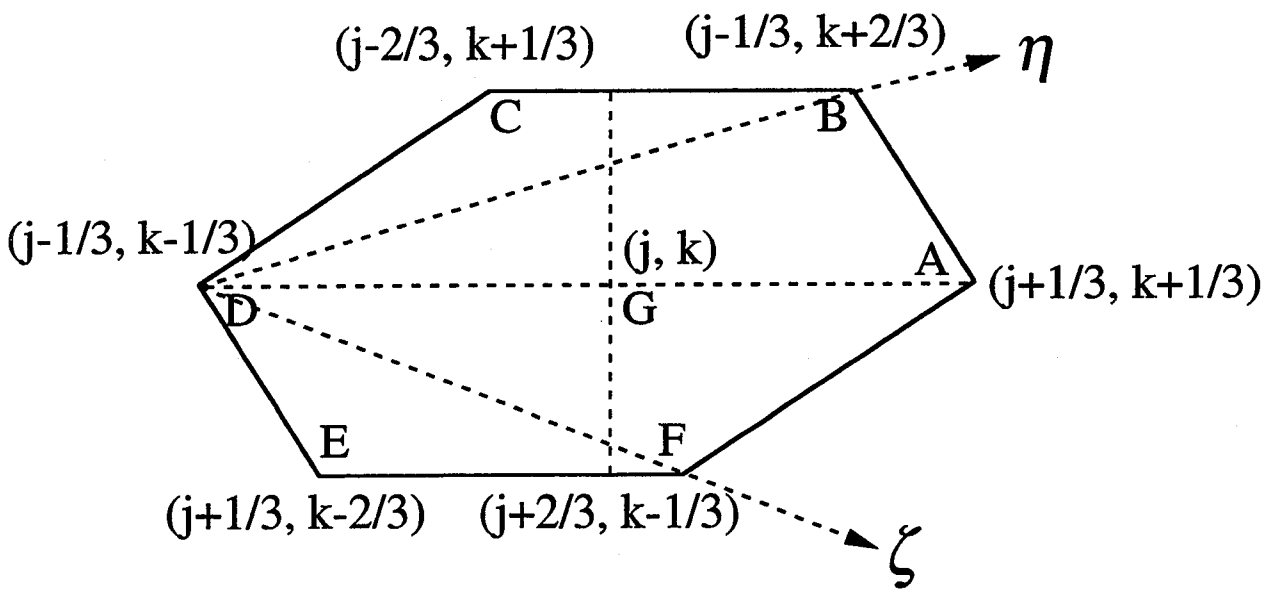

(f) The hexagon ABCDEF, the coordinate (ζ ,η) and the parameters w, b and h.

Fig. 1 Concluded.

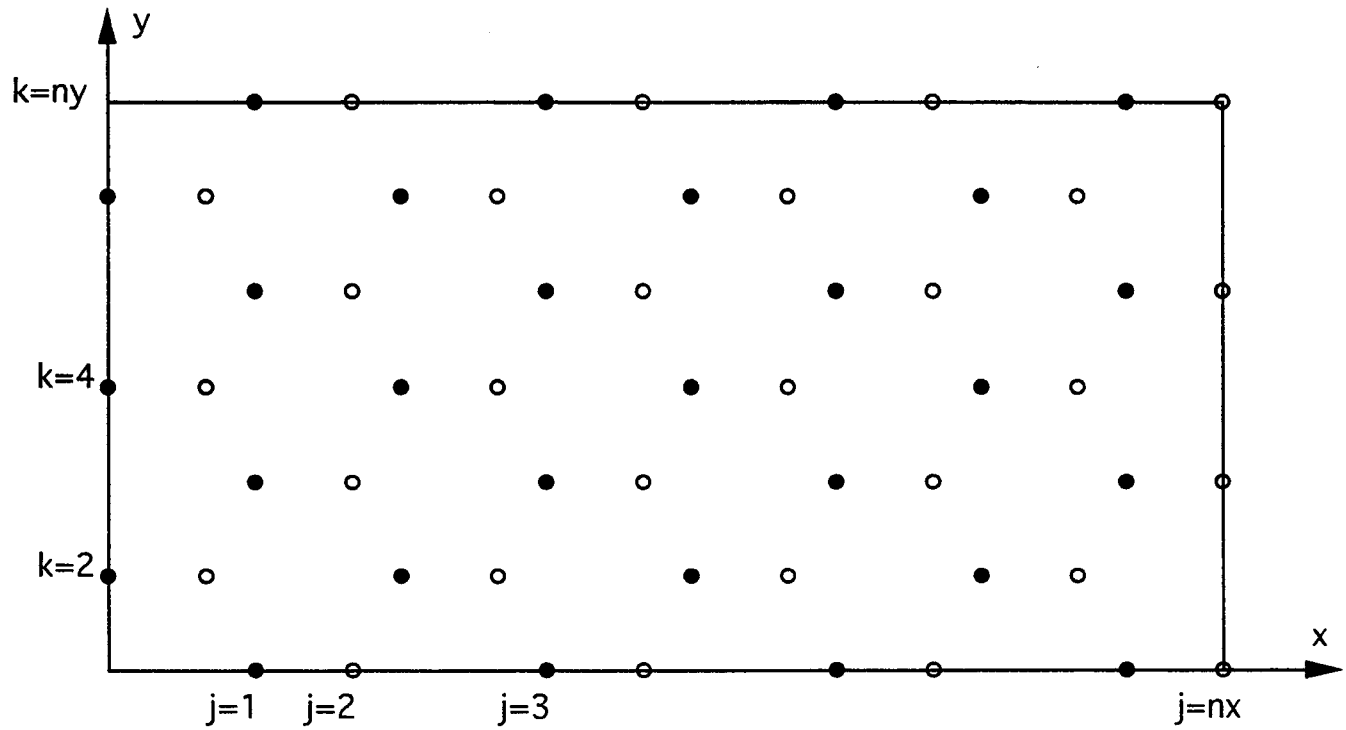

nx is an even integer. ny is an odd integer.

- ○ at time levels n=2, 4, 6,....
- ● at time levels n=1, 3, 5,....

(a) The relative position of the mesh points

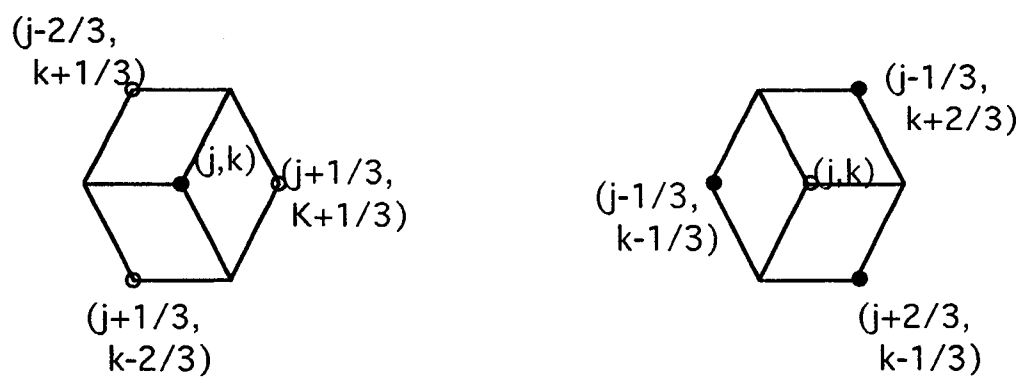

(b) Projected view of the interior CEs

Fig. 2 The grid point distribution, the interior and boundary CEs used for solving the diffusion equation

(c) Projected view of the boundary CEs at x=0 and x=1

(d) Projected view of the boundary CEs at y=0

(e) Projected view of the boundary CEs at y=1

Fig. 2 Concluded.

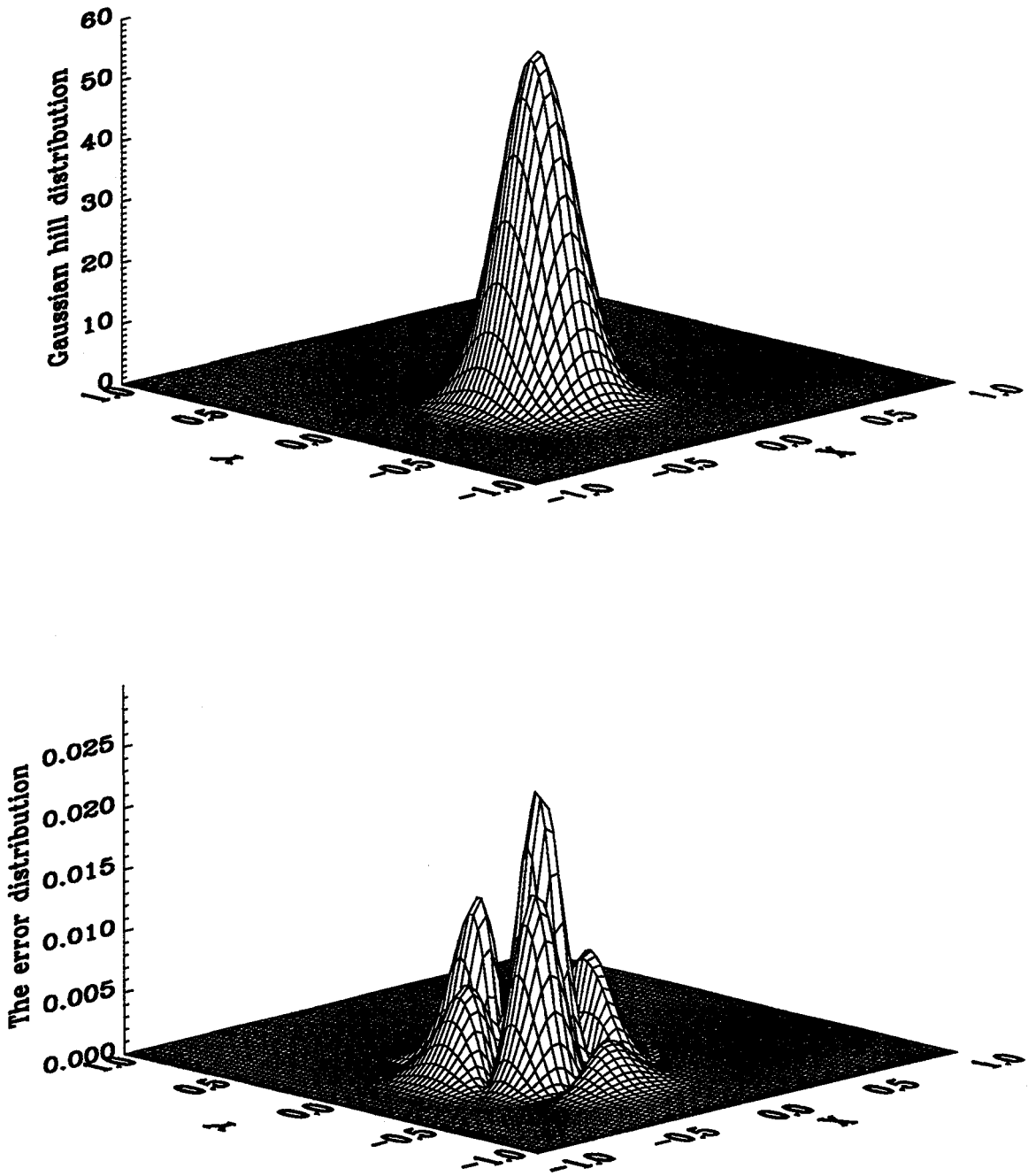

Fig. 3 The CE/SE solution and error distribution($n = 50, m = 173, \Delta t = 0.005$) **at t=0.5 for** $\nu = 0.0125$

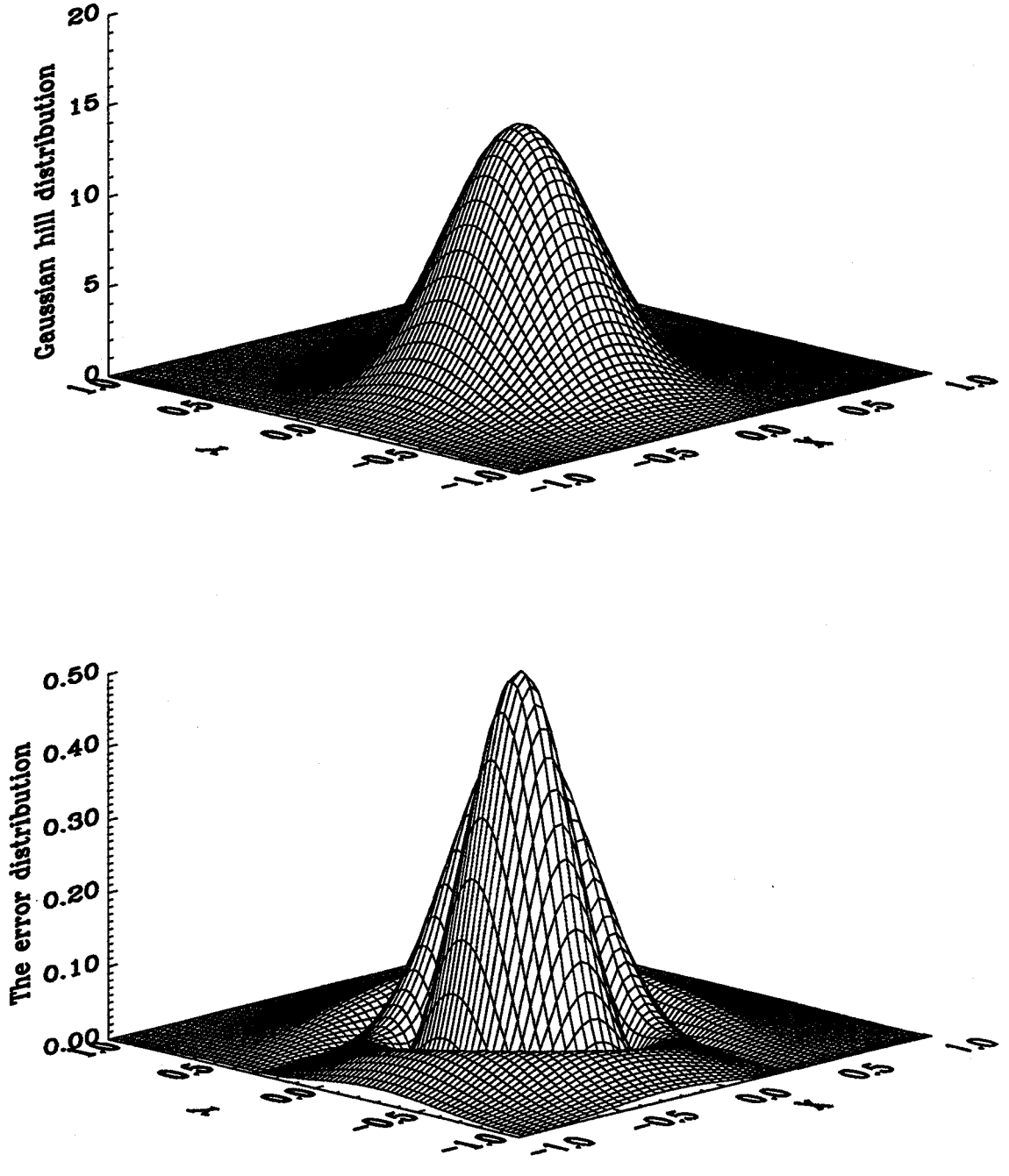

Fig. 4 The CE/SE solution and error distribution($n = 50, m = 173, \Delta t = 0.005$) at t=0.5 for $\nu = 0.0625$

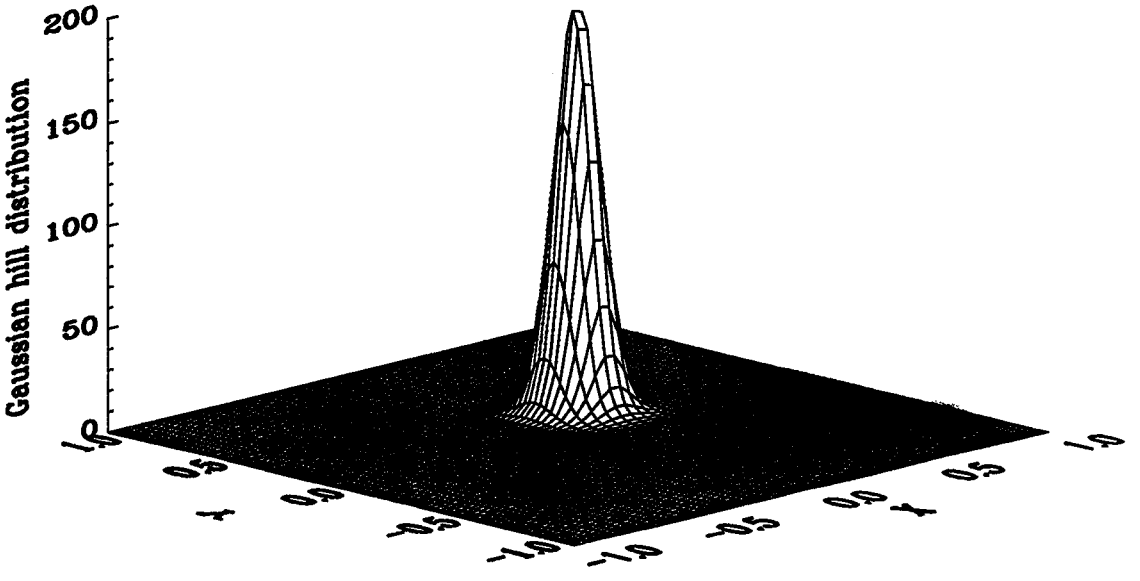

Fig. 5(a) The exact solution of purely advecting Gaussian hill at t=1.0.

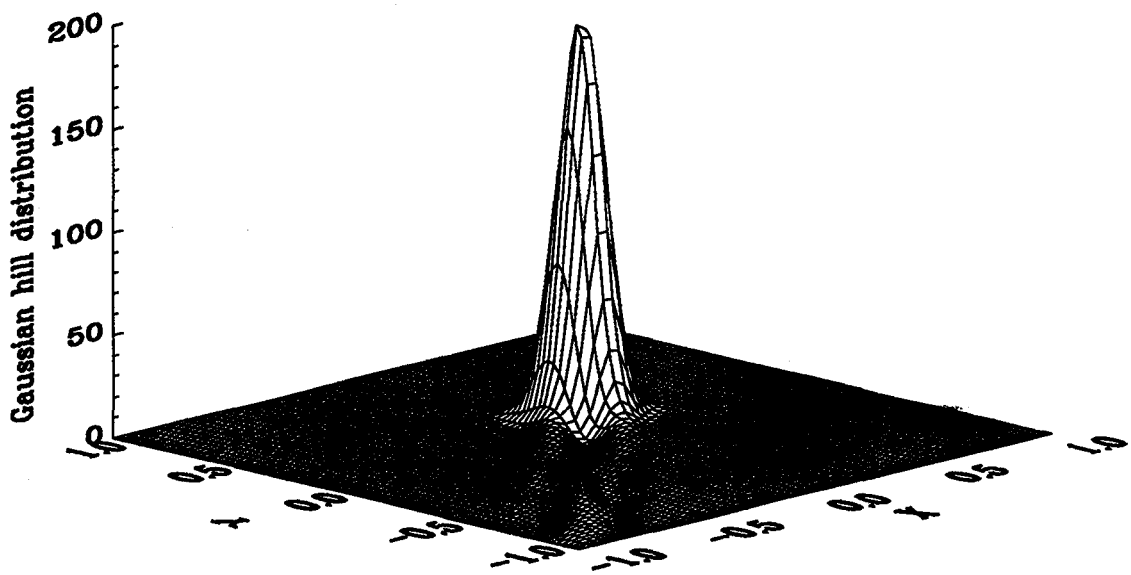

Fig. 5(b) The CE/SE solution($n = 50$, $m = 173$, $\epsilon = 0$, $\Delta t = 0.02$) **of purely advecting Gaussian hill at t=1.0.**

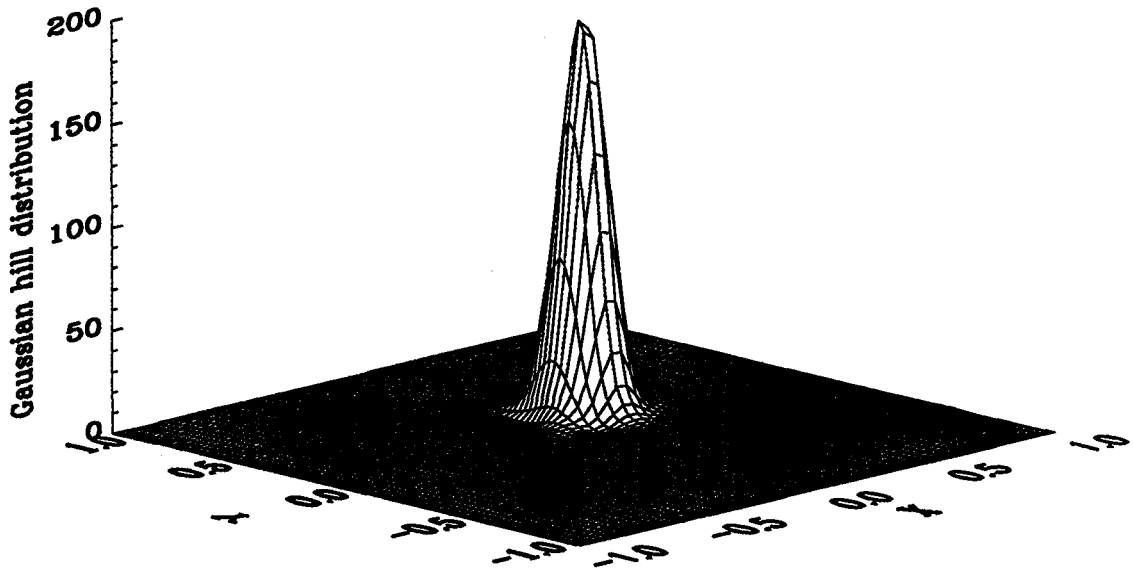

Fig. 5(c) The CE/SE solution($n = 50, m = 173, \epsilon = 0.1, \Delta t = 0.02$) **of purely advecting Gaussian hill at t=1.0.**

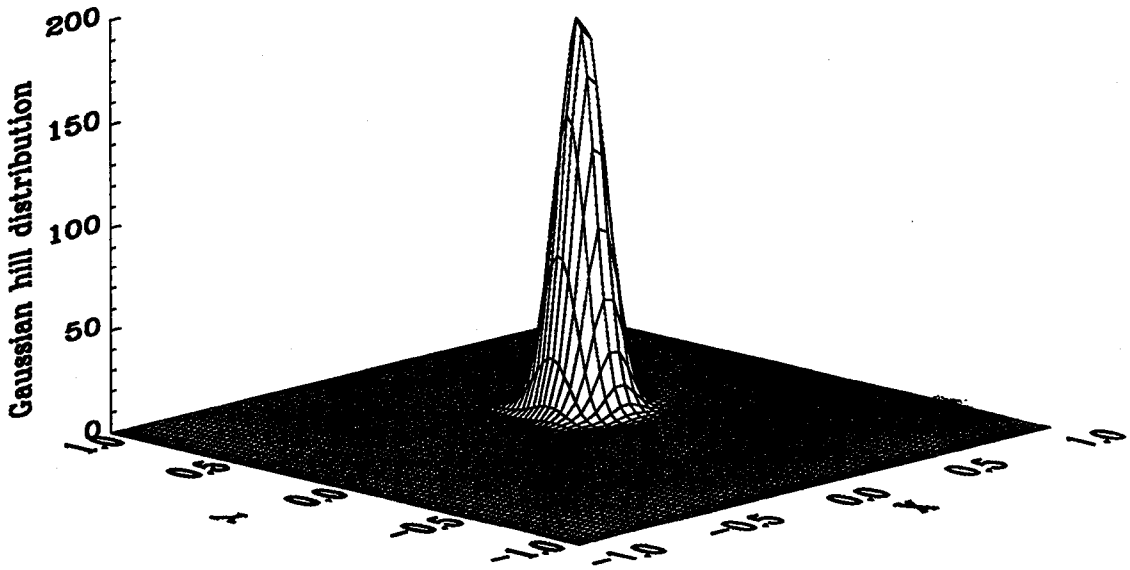

Fig. 5(d) The CE/SE solution($n = 50, m = 173, \epsilon = 0.3, \Delta t = 0.02$) **of purely advecting Gaussian hill at t=1.0.**

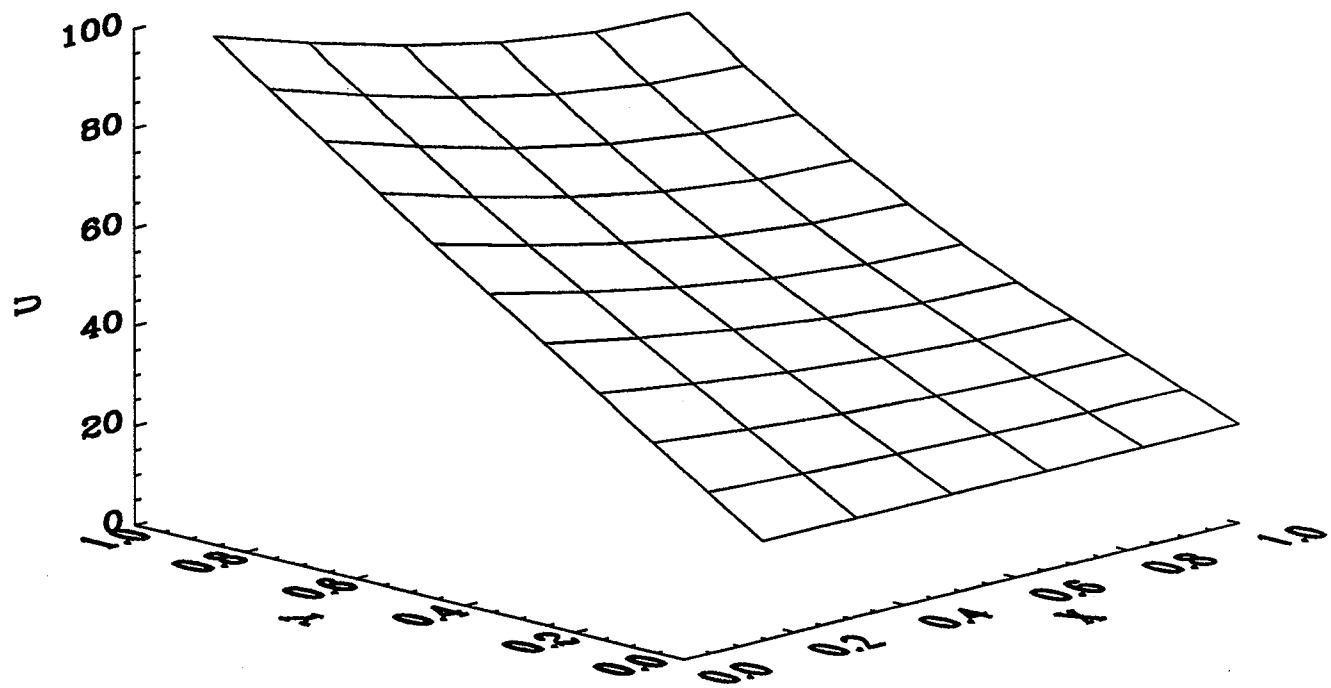

Fig. 6 The CE/SE solution($n = 6$, $m = 21$, $\Delta t = 100$) of diffusion equation at t=24000.

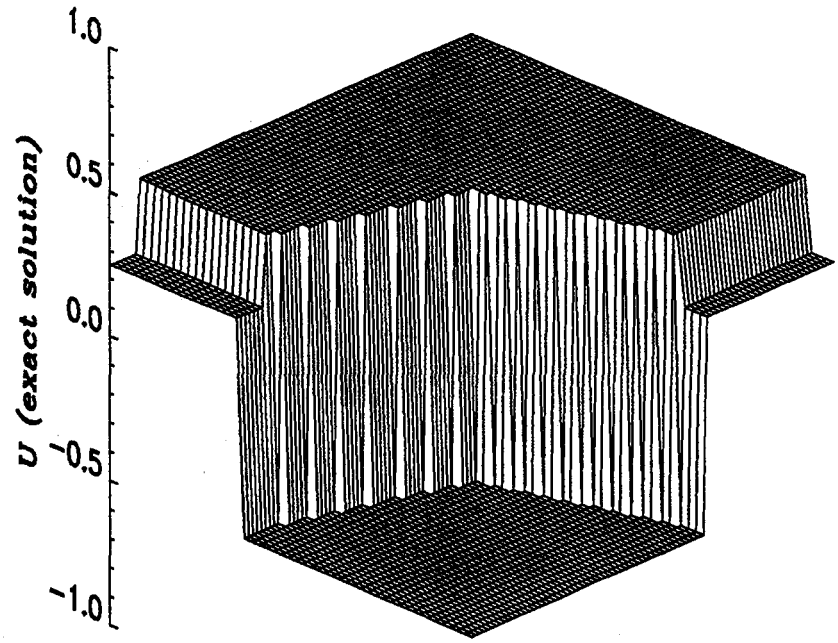

Fig. 7(a) The exact solution of the inviscid Burgers equation at t=1.125 for the first case.

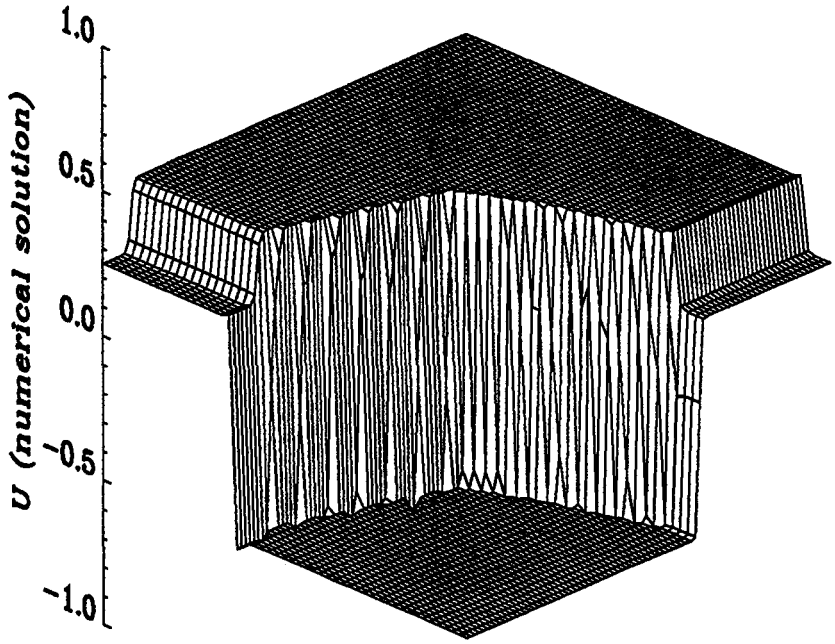

Fig. 7(b) The CE/SE solution ($n = 50$, $m = 173$, $\epsilon = 0.5$, $\alpha = 1$, $\Delta t = 0.01$) **of the inviscid Burgers equation at t=1.125 for the first case.**

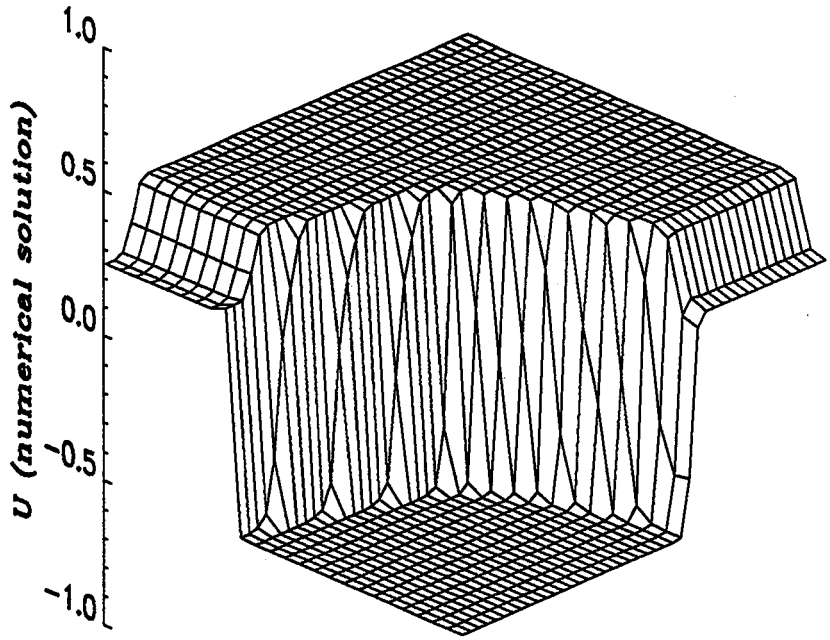

Fig. 7(c) The CE/SE solution ($n = 25, m = 87, \epsilon = 0.5, \alpha = 1, \Delta t = 0.01$) **of the inviscid Burgers equation at t=1.125 for the first case.**

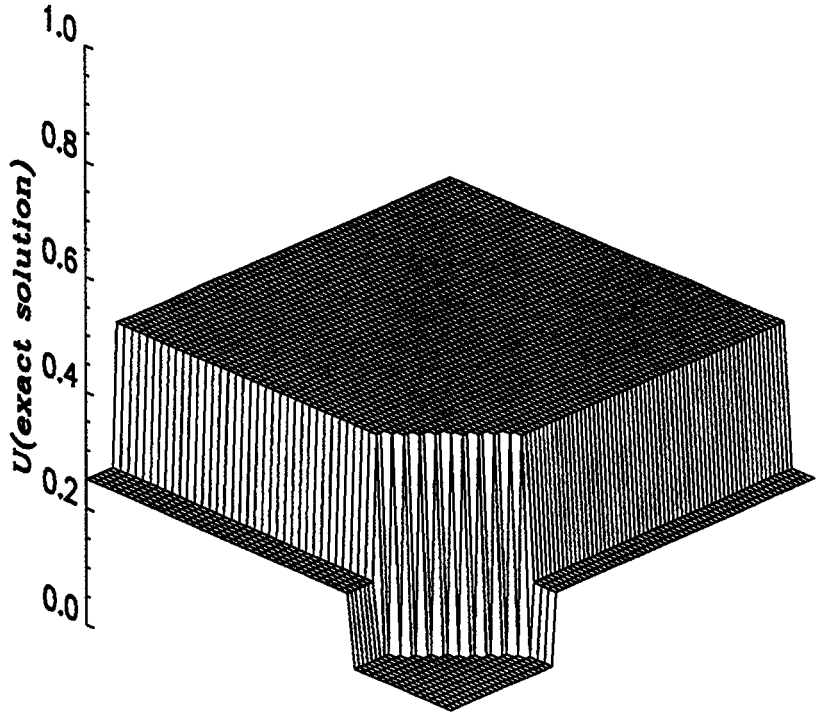

Fig. 8(a) The exact solution of the inviscid Burgers equation at t=1.125 for the second case.

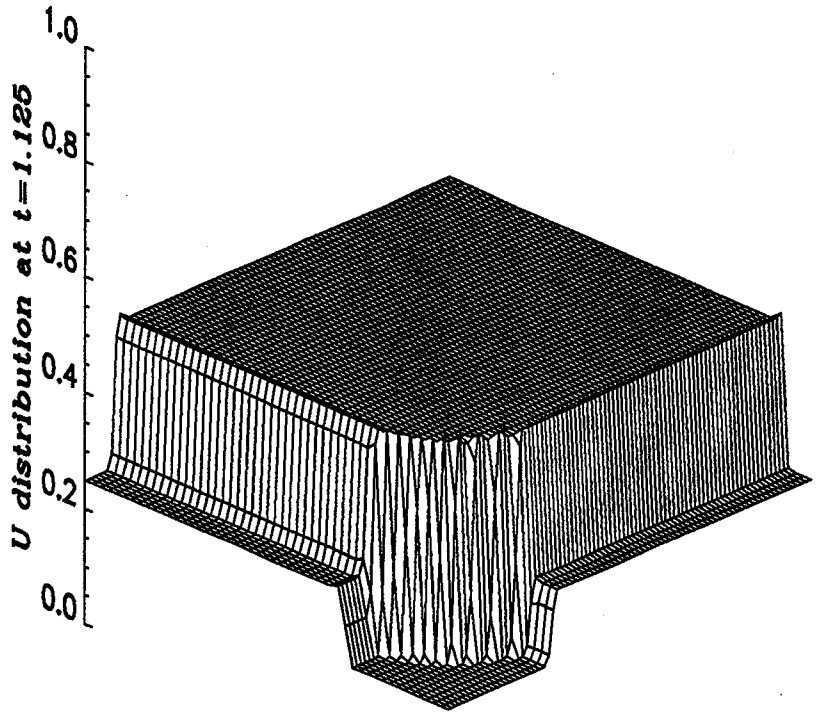

Fig. 8(b) The CE/SE solution ($n = 50$, $m = 173$, $\epsilon = 0.5$, $\alpha = 1/2$, $\Delta t = 0.01$) **of the inviscid Burgers equation at t=1.125 for the second case.**

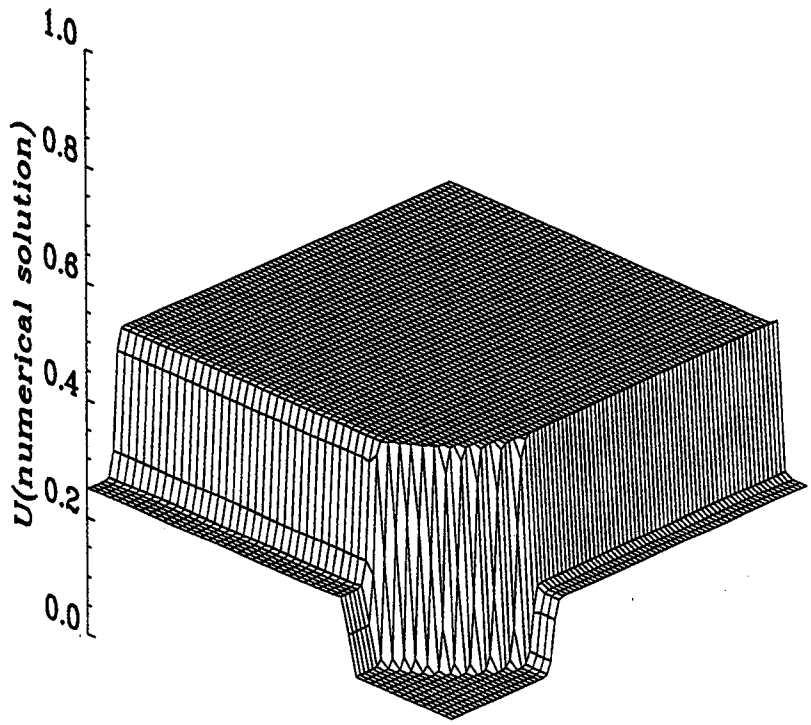

Fig. 8(c) The CE/SE solution ($n = 50, m = 173, \epsilon = 0.5, \alpha = 1, \Delta t = 0.01$) **of the inviscid Burgers equation at t=1.125 for the second case.**

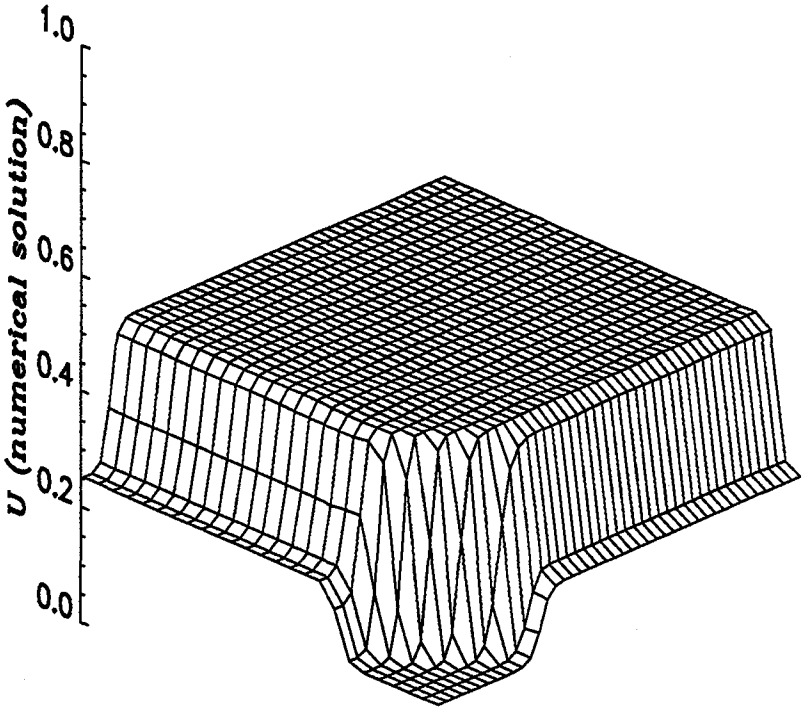

Fig. 8(d) The CE/SE solution ($n = 25, m = 87, \epsilon = 0.5, \alpha = 1, \Delta t = 0.01$) **of the inviscid Burgers equation at t=1.125 for the second case.**

REPORT DOCUMENTATION PAGE

Form Approved
OMB No. 0704-0188

1. AGENCY USE ONLY (*Leave blank*)	2. REPORT DATE	3. REPORT TYPE AND DATES COVERED
	June 1995	Technical Memorandum

4. TITLE AND SUBTITLE

Application of the Space-Time Conservation Element and Solution Element Method to Two-Dimensional Advection-Diffusion Problems

5. FUNDING NUMBERS

WU-505-62-52

6. AUTHOR(S)

Xiao-Yen Wang, Chuen-Yen Chow, and Sin-Chung Chang

7. PERFORMING ORGANIZATION NAME(S) AND ADDRESS(ES)

National Aeronautics and Space Administration
Lewis Research Center
Cleveland, Ohio 44135-3191

8. PERFORMING ORGANIZATION REPORT NUMBER

E-9681

9. SPONSORING/MONITORING AGENCY NAME(S) AND ADDRESS(ES)

National Aeronautics and Space Administration
Washington, D.C. 20546-0001

10. SPONSORING/MONITORING AGENCY REPORT NUMBER

NASA TM-106946

11. SUPPLEMENTARY NOTES

Xiao-Yen Wang and Chuen-Yen Chow, University of Colorado, Department of Aerospace Engineering Sciences, Boulder, Colorado 80309-0429 (work funded by NASA Grant NAG3-1566), and Sin-Chung Chang, NASA Lewis Research Center. Responsible person, Sin-Chung Chang, organization code 2660, (216) 433-5874.

12a. DISTRIBUTION/AVAILABILITY STATEMENT

Unclassified - Unlimited
Subject Categories 64 and 34

This publication is available from the NASA Center for Aerospace Information, (301) 621-0390.

12b. DISTRIBUTION CODE

13. ABSTRACT (*Maximum 200 words*)

The existing 2-D a-μ scheme and a-ϵ scheme based on the method of space-time conservation element and solution element, which were constructed for solving the linear 2-D unsteady advection-diffusion equation and unsteady advection equation, respectively, are tested here. Also, the a-ϵ scheme is modified here to become the v-ϵ scheme for solving the nonlinear 2-D inviscid Burgers equation. Numerical solutions of six test problems are presented in comparison with their exact solutions or numerical solutions obtained by traditional finite-difference or finite-element methods. It is demonstrated that the 2-D a-μ, a-ϵ and v-ϵ schemes can be used to obtain numerical results which are more accurate than those based on some of the traditional methods but without using any artificial tuning in the computation. Similar to the previous 1-D test problems, the high accuracy and simplicity features of the space-time conservation element and solution element method have been revealed again in the present 2-D test results.

14. SUBJECT TERMS

Space-time; Conservation element; Solution element; Two-dimensional; Advection-diffusion problems

15. NUMBER OF PAGES

45

16. PRICE CODE

A03

17. SECURITY CLASSIFICATION OF REPORT	18. SECURITY CLASSIFICATION OF THIS PAGE	19. SECURITY CLASSIFICATION OF ABSTRACT	20. LIMITATION OF ABSTRACT
Unclassified	Unclassified	Unclassified	

National Aeronautics and
Space Administration

Lewis Research Center
21000 Brookpark Rd.
Cleveland, OH 44135-3191